DOI:10.14753/SE.2016.1927

APPLICABILITY OF ROTARY SPUN HYDROXYPROPYL CELLULOSE MICROFIBERS FOR THE FORMULATION OF ORODISPERSIBLE TABLETS OF POORLY SOLUBLE DRUGS

Ph.D. thesis

Péter Szabó

Doctoral School of Pharmaceutical Sciences

Semmelweis University

Supervisor: Dr. Romána Zelkó, D.Sc., professor

Official reviewers:
Dr. Ildikó Kovácsné Bácskay, Ph.D., associate professor
Dr. Krisztina Ludányi, Ph.D., associate professor

Head of the Final Examination Committee:
Dr. Krisztina Takácsné Novák, D.Sc., professor

Members of the Final Examination Committee:
Dr. Piroska Révész, D.Sc., professor
Dr. Lívia Budai, Ph.D., assistant professor

Budapest
2016

DOI:10.14753/SE.2016.1927

1. TABLE OF CONTENTS

DOI:10.14753/SE.2016.1927

DOI:10.14753/SE.2016.1927

2. LIST OF ABBREVIATIONS

A	-	surface area
Å	-	ångström
$A_{diss,n}$	-	dissolved amount of a solute at the n-th segment of the gastrointestinal tract
ADMET	-	absorption, distribution, metabolism, excretion and toxicity
ASD	-	amorphous solid dispersion
ATR-FTIR	-	attenuated total reflectance - Fourier transform infrared
BCS	-	Biopharmaceutical Classification System
Bq	-	becquerel
C	-	concentration
°C	-	degree Celsius
Ca	-	capillary number
CD	-	carvedilol
CDER	-	Center for Drug Evaluation and Research
C_s	-	saturation concentration
$C_{s,n}$	-	solubility of the compound at the particle surface at the n-th segment of the gastrointestinal tract
Cu	-	copper
D	-	diffusion coefficient
$D_{10\%}$	-	the particle size at the intercept of the cumulative distribution curve and 10%
$D_{50\%}$	-	median diameter, or the particle size at the intercept of the cumulative distribution curve and 50%
$D_{90\%}$	-	the particle size at the intercept of the cumulative distribution curve and 90%
Δr	-	electron layer thickness, equals to 1.66 Å
DSC	-	differential scanning calorimetry
η	-	dynamic viscosity
$E_{Cavitation}$	-	cavitation energy
ECM	-	extracellular matric
$E_{Crystal\ Packing}$	-	crystal packing energy

$E_{Solvation}$	-	solvation energy
f_1	-	difference factor
f_2	-	similarity factor
F_{Cent}	-	centrifugal force
FDA	-	U.S. Food and Drug Administration
FTIR	-	Fourier transform infrared spectroscopy
γ_{sl}	-	solid-liquid interfacial tension
g	-	Gram
GI	-	gastro-intestinal
GIT	-	gastro-intestinal tract
h	-	thickness of the diffusion layer
h_{app}	-	apparent diffusion layer thickness
HPC	-	hydroxypropyl cellulose
k_B	-	Boltzmann constant, equals to $1.38x10^{-23}$ JK^{-1}
kV	-	kilovolt
λ	-	wavelength
logP	-	logarithm of partition coefficient
m	-	mass
M	-	molar (molar concentration)
M_w	-	molecular weight
mA	-	milliamper
MD	-	model drug
MPa	-	megapascal
µg	-	microgram
mg	-	milligram
min	-	minute
mJ	-	millijoule
ml	-	millilitre
mm	-	millimetre
N	-	newton
nA	-	nanoamper
ω	-	angular velocity

o-Ps	-	ortho-positronium
π	-	pi, mathematical constant, approximately 3.14159
PALS	-	positron annihilation lifetime spectroscopy
pH	-	pondus hydrogenii
pKa	-	acid dissociation constant
ps	-	picosecond
r	-	radius
R	-	universal gas constant, equals to 8.314 $JK^{-1}mol^{-1}$
ρ	-	volumetric mass density
RH	-	relative humidity
rpm	-	revolutions per minute
R_t	-	dissolution value of reference at t time
s	-	second
S	-	solubility
S_∞	-	normal solubility of a material with a plane surface
SEM	-	scanning electron microscope
S_r	-	solubility of a particle of r radius
SS	-	solid solution
t	-	time
τ_3	-	ortho-positronium lifetime
T	-	temperature
T_t	-	dissolution value of test at t time
U	-	polymer jet exit speed
v	-	number of ions dissociating from the solute
V	-	volume of dissolution medium
$V_{lumen,n}$	-	volume of the liquid presented in the n-th segment of the gastrointestinal tract
% v/v	-	volume concentration
% w/w	-	mass fraction, percentage by mass
XRD	-	powder X-ray diffraction

DOI:10.14753/SE.2016.1927

3. INTRODUCTION

Recent trends in pharmaceutical industry enforce the consideration of novel dosage forms in course of the development of pharmaceutically active ingredients. The phenomenon of the increasing demands for special therapeutic purposes and the expanding proportion of actives of undesirable physicochemical properties have been of the major concerns for pharmaceutical researchers. A widely accepted approach for classifying pharmaceuticals is the biopharmaceutical drug classification system (BCS) in which actives are categorized based on their solubility and permeability is represented in Fig. 1 (Amidon *et al.*, 1995).

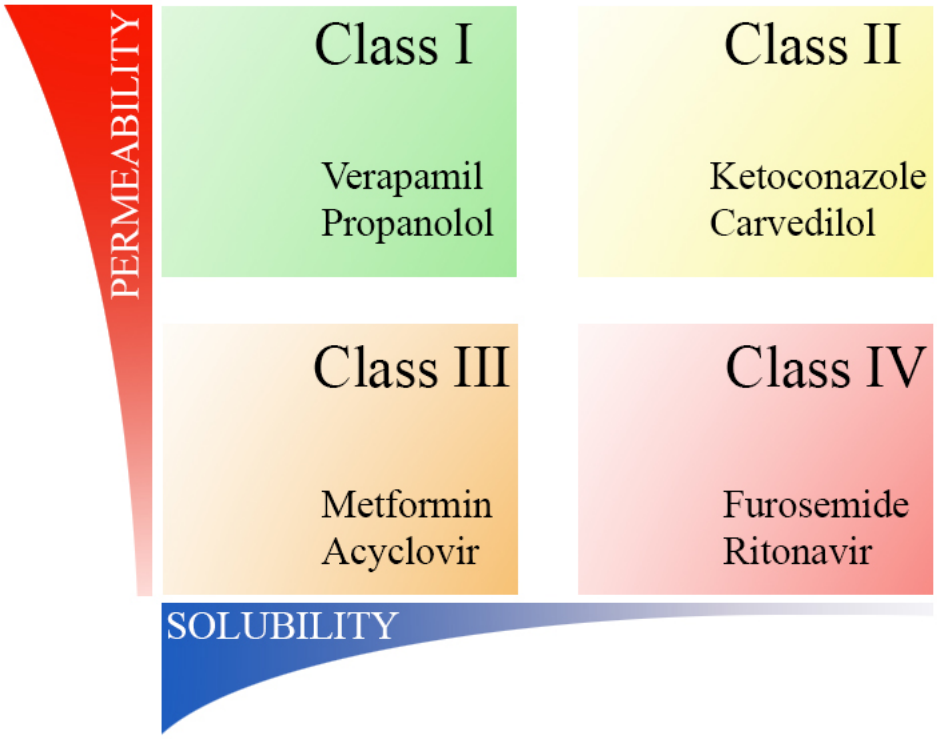

Figure 1 Illustration of Biopharmaceutical Classification System including typical representatives of each class

As can be seen from Fig. 1, members of class I possess the most advantageous physicochemical features enabling their rapid and complete dissolution and absorption. The general view is that formulation is an effective way to improve the gastrointestinal behavior of drugs belonging to class II, while chemical modification should be considered for actives of classes III and IV (Pouton, 2006). A remarkable part of these formulations

focuses on the dissolution and solubility enhancement of the incorporated ingredients. However, it can be noted that several research papers were published turning the spotlight on the permeation and bioavailability improvement of drugs of class III and IV (Kaukonen *et al.*, 2007; Özdemir *et al.*, 2000; Sinha *et al.*, 2010; Yu *et al.*, 1999). Moreover, the assessment of class II drugs is further complicated since it has been demonstrated that an enhanced in vitro dissolution does not result necessarily in an increased oral bioavailability (Sarnes *et al.*, 2014). Another crucial obstacle is that formulations usually cannot address such phenomenon as high rate of metabolism or extensive efflux transport associated with class II-IV drugs (Wu and Benet, 2005).

The real problem lies in the ever-decreasing number of approvals of new chemical entities, which is partly believed as a consequence of the extensive proportion of drugs of unfavorable physicochemical features (Fig. 2).

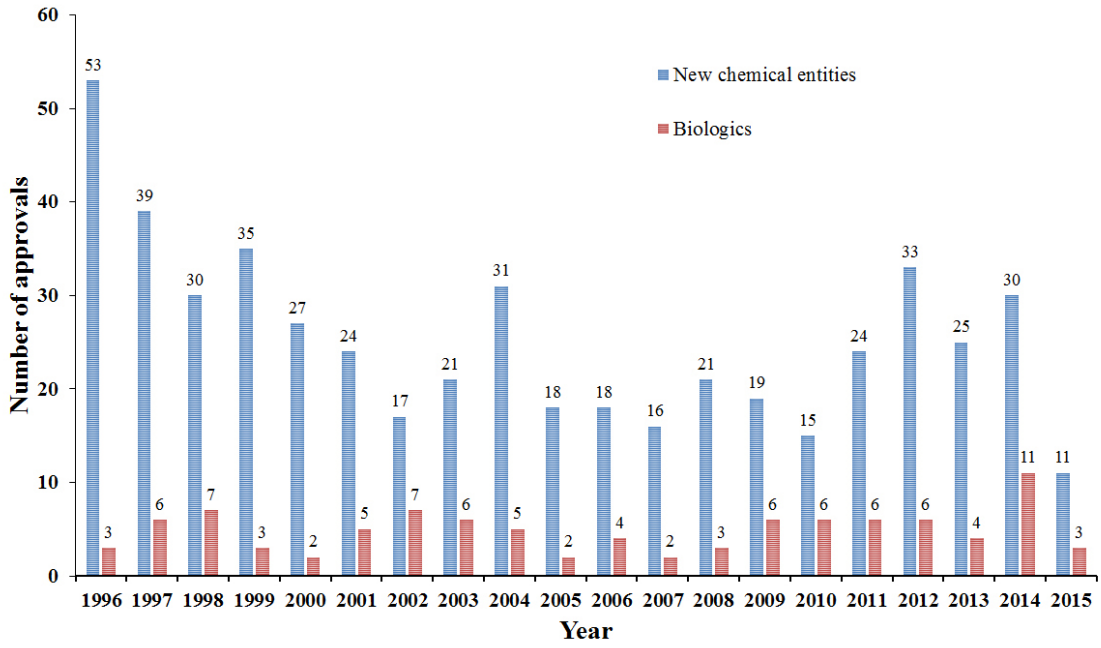

Figure 2 Number of original drug approvals per year by FDA (FDA, 2016)

The root of this tendency lies in the regnant approaches in modern drug development: the rational drug discovery and the high throughput screening lead to poorer permeability and poorer solubility, respectively (Lipinski, 2000). Hann *et al.* have identified this issue as the aftermath of the upset balance between potency and ADMET features resulting in molecular obesity. This term refers to the large molecular size and lipophilicity, as well

as the poor aqueous solubility of the actives (Hann, 2011; Hann and Keseru, 2012). Against this background, it is not surprising that approximately 70% of new chemical entities and 30% of marketed drugs belong to the BCS class II (Wu and Kesisoglou, 2010). The reason why the proportion of BCS class II drugs is smaller among marketed drugs is that such molecules had been neglected during the early development stages.

3.1. Solubility and the rate of dissolution

In physical chemistry, two kinds of solubilities can be distinguished: the thermodynamic solubility and the kinetic solubility. The thermodynamic solubility refers to a physically long-term stable condition, and can be described as the concentration of a solute in a solution in equilibrium with the normal sized powder of the most stable crystalline state. The kinetic solubility is not a physically long-term stable condition and is defined as the concentration of a solute in a solution in equilibrium with a metastable crystalline state. The kinetic solubility is usually higher than thermodynamic solubility (Janssens and Van den Mooter, 2009; Mauludin *et al.*, 2009).

Generally, three quantities have been recognized, which affect the solubility (S) of a drug, and their relationship with solubility is described in the following equation:

$$S = f(E_{Crystal\ Packing} + E_{Cavitation} + E_{Solvation}) \qquad (1)$$

where $E_{Crystal\ Packing}$ refers to the endoergic energy responsible for the disruption of the crystalline lattice in order to remove molecules from. $E_{Cavitation}$ means the endoergic energy related to the disruption of the water molecules creating a cavity suitable to host the solute, and $E_{Solvation}$ represents the resultant energy deriving from the interactions of the solute and the solvent (Lipinski *et al.*, 2012).

The applied solvent, solvent mixture, the temperature, pH, solid state, ionic strength are the main parameters affecting the solubility of a given compound (Stegemann *et al.*, 2007).

Another important characteristic of the drug liberation is the rate of dissolution, which is equivalent to the amount of drug dissolved per unit time. Noyes and Whitney described

the proportionality between the dissolution rate and the difference of the concentration of the saturated solution and the solution in question (Noyes and Whitney, 1897).

Later on, Nernst and Brunner published an improved equation (Eq. (2)) on the basis of the diffusion layer approach:

$$\frac{dC}{dt} = \frac{DA}{Vh}(C_S - C) \tag{2}$$

where D is the diffusion coefficient, A the surface area of the interface between the compound to be solved and the solution, V the volume of the dissolution medium, h the thickness of the diffusion layer, C_S the saturation solubility and C the concentration of the solute in the bulk phase at t time (Brunner, 1904; Dokoumetzidis and Macheras, 2006; Nernst, 1904).

Regarding the huge number of research papers focusing on particle size reduction and the formulation of nanoscale drug delivery systems it is essential to discuss the impact of particle size and interfacial tension on the solubility. The dependence of the saturation solubility on the particle size was given by Ostwald and Freundlich (Eq. (3)):

$$\rho v \frac{RT}{M_w} ln \frac{S_r}{S_\infty} = \frac{2\gamma_{sl}}{r} \tag{3}$$

where ρ is the volumetric mass density, r the radius of the particles, v represents the number of ions dissociating from the solute, M the molecular weight of the solute, γ_{sl} the solid-liquid interfacial tension, R the ideal gas constant, T the temperature S_r and S_∞ the solubility of the particle of r radius and the normal solubility of a plane surface, respectively (Wu and Nancollas, 1998). In other words, the solubility of a compound of a given particle size changes exponentially with the reciprocal radius. However, it must be noted that the particle size reduction related solubility enhancement is significant only below a particle size of 2 μm and even more below 1 μm (Müller *et al.*, 2000).

Since Eqs. 2 and 3 are applicable only in the existence of a steady state condition suggesting a linear concentration gradient along with the diffusion layer, Wang and Flanagan introduced a new equation taking into account that the dissolution rate is influenced by the surface curvature and that the width of apparent diffusion layer alters

with change of the particle size. The authors proposed that in case of monodispersed spherical particles, *h* in Eq. (2) should be replaced with h_{app}, the apparent diffusion layer thickness, which was given as

$$\frac{1}{h_{app}} = \frac{1}{h} + \frac{1}{r} \tag{4}$$

where *h* is the diffusion layer thickness, and *r* the particle radius (Wang and Flanagan, 1999, 2002).

Based on these considerations, to describe in vivo conditions, the following equation (Eq. (5)) can be defined:

$$\frac{dA_{diss,n}}{dt} = -4\pi r^2(t) D \left(\frac{1}{r(t)} + \frac{1}{h}\right)\left(C_{s,n} - \frac{A_{diss,n}}{V_{lumen,n}(t)}\right) \tag{5}$$

where, $dA_{diss,n}/dt$ is the dissolution rate of the particle of *r(t)* radius at *t* time, *D* the diffusion coefficient, *h* the diffusion layer thickness, $C_{s,n}$ the compound solubility at the partice surface, $A_{diss,n}$ the dissolved amount of the solute, and V_{lumen} the volume of the liquid presented in the *n*-th segment of the gastrointestinal tract (GIT) (Jamei *et al.*, 2009).

3.1.1. The biopharmaceutical aspects of solubility

Though there are some exceptions (active or the paracellular transport), the vast majority of the active ingredients is absorbed from the GIT via passive diffusion (Bravo-Osuna *et al.*, 2008). The generally accepted model for the gastrointestinal absorption of these drugs requires for dissolved active compound at the absorption sites (Jamei *et al.*, 2009; Rao *et al.*, 2009; van De Waterbeemd *et al.*, 2001). Two main scenario can be classified on this basis. One is that when the drug remains undissolved at the window of absorption because of its poor solubility. The other is that when the rate of dissolution is too low, therefore the transit time is not sufficient for the complete dissolution and solid drug particles pass through the absorption site (Hörter and Dressman, 2001).

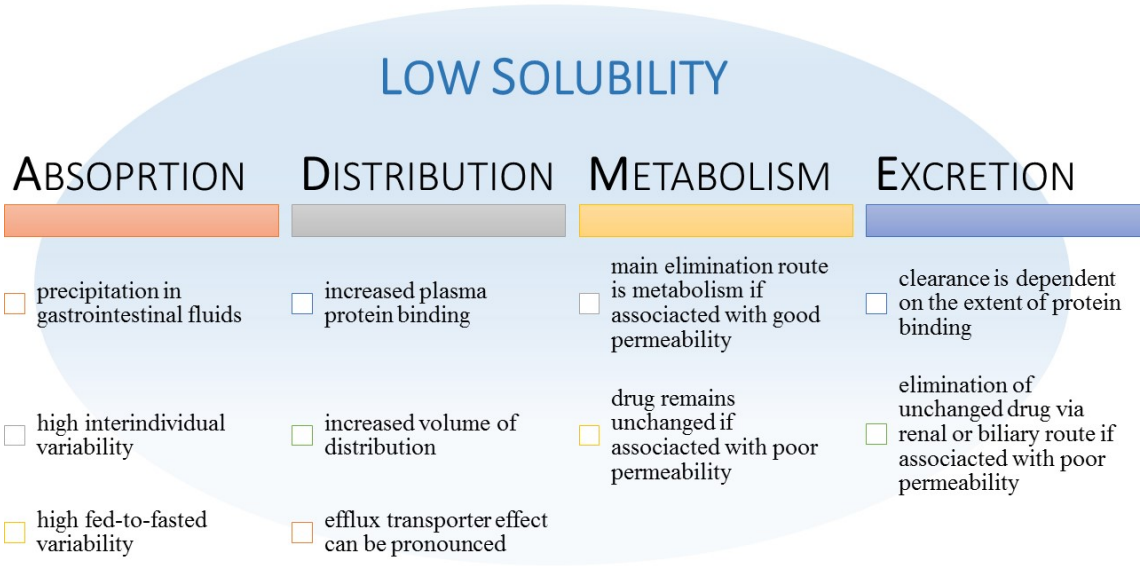

Figure 3 The relationship of poor solubility and the ADME scheme (Leach *et al.*, 2006; Merisko-Liversidge and Liversidge, 2011; Wu and Benet, 2005)

The most pronounced effect of inadequate solubility features is the low bioavailability. Alongside with the absorption issue, difficulties of the lead optimization and dosing are not negligible, as well. Furthermore, such active compounds often call for innovative dosage forms comprising excipients which are not indifferent to the human body. Additionally, these approaches often try to ameliorate poor solubility properties by the kinetic solubility using a dosage form containing drugs in a metastable state (e.g. amorphous state). Since the kinetic solubility is not a long-term stable condition and uncontrollable precipitation can occur, large variabilities of bioavailability can be expected. Parenteral and other dosage forms associated with discomfort and complication at administration can result in a diminished patients' compliance (Kayser *et al.*, 2003; Merisko-Liversidge and Liversidge, 2011). With respect to acidic compounds, the formulation of an immediate release dosage forms can be arduous because of the dissolution hampering and precipitation facilitating effect of the acidic media in the upper tracts of the GIT (Maggi *et al.*, 2015).

Fig. 3 illustrates how poor aqueous solubility influences the fate of drugs in the human body (Leach *et al.*, 2006; Merisko-Liversidge and Liversidge, 2011; Wu and Benet, 2005).

Finally, it is important to emphasize the significance of the proper physicochemical and biological characterization of the actives. This is especially interesting for drugs, where low oral exposure is attributed to the poor aqueous solubility, whilst intensive efflux or presystemic metabolic activity are behind the phenomenon, thus low solubility veils poor permeability feature (Stella and Nti-Addae, 2007). Cyclosporine represents a typical example, where formerly the low oral performance was assigned to its poor aqueous solubility and high lipophilicity. Further investigations revealed that the real extent of absorption exceeds much more the presumed value and indicated that the observed low oral bioavailability is a consequence of the intestinal metabolism (Benet *et al.*, 1996; Hebert *et al.*, 1992; Wu *et al.*, 1995).

3.2. Pharmaceutical strategies to overcome poor solubility in solid dosage forms

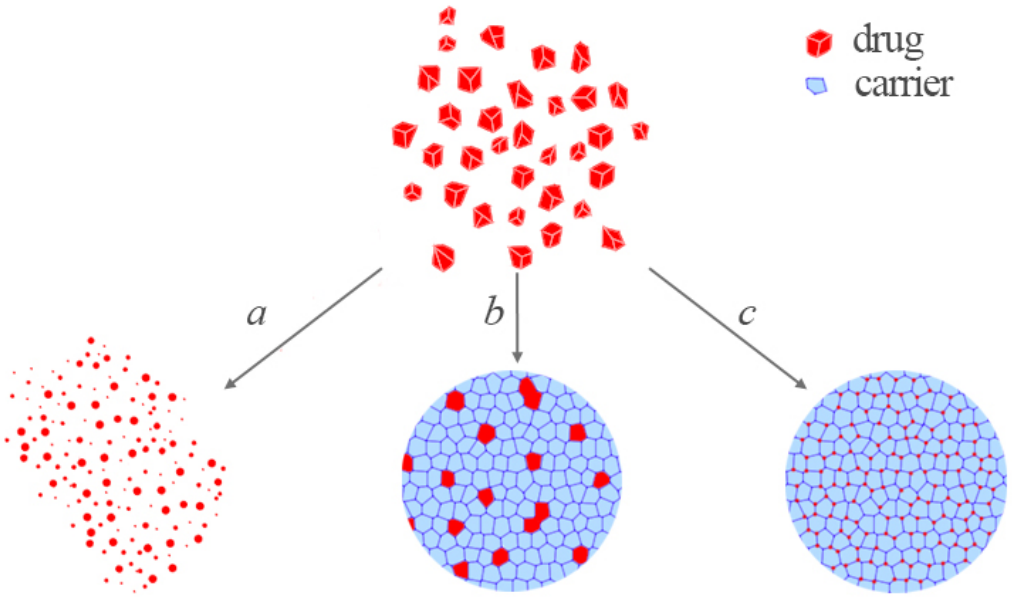

Figure 4 Structural differences of the main approaches for the dissolution enhancement of poorly soluble drugs: a) particle size reduction, b) amorphous drug dispersion c) solid solutions

Apart from chemical approaches, *e.g.* pH adjustment, salt formation, complexation or the prodrug strategy, the most important means of overcoming the solubility issue are still resting on the basis of physical principles. Therefore this chapter focuses on approaches based on physical methods for improving solubility.

As can be seen in Fig. 4, the three major approaches of such efforts are the particle size reduction, the formation of amorphous dispersions and solid solutions.

3.2.1. Particle size reduction

Particle size reduction is a long-standing way of handling poorly soluble drugs. Lowering particle radius influences diffusion coefficient, lessens diffusion layer thickness (Eq. (4)) and increases concentration gradient, thus manifesting as an increment of dissolution rate and as the improvement of solubility, as well. The lower the particle radius the larger the diffusion coefficient according to Eq. (6) known as the Stokes-Einstein relationship:

$$D = \frac{k_B T}{6\pi\eta r} \tag{6}$$

where r is the radius of the spherical particle, k_B is Boltzmann's constant, T is the temperature and η is the dynamic viscosity of the solution (Edward, 1970). Based on Eq. (2) it is easy to see that dissolution rate is directly proportional to the particle size dependent diffusion coefficient.

In case of an appropriate extent of size reduction, *i.e.* particle radius below 1 μm, the solubility surplus can reach such degree, which allows the formulation of poorly soluble compounds (Eq. (3)).

There are a great number of particle size reducing methods, which can be classified in two groups, the bottom up and the top down techniques. In the instance of bottom up approaches, fine particles are obtained from a homogenous system (usually solutions) exposed to a physical or chemical trigger. The latter refers to techniques, which scale down particle radius by means of mechanical or other physical energy. The conventional methods for particle size reduction are listed in Table 1.

Table 1 Overview of the particle size reducing techniques

	Benefits	**Drawbacks**	Reference
Top Down Methods			
Milling	basic and easy technology, time-saving, solvent free	physical and thermal stress can induce drug degradation, erosion from milling pearls	(Keck and Müller, 2006; Savjani *et al.*, 2012)
High pressure homogenization	simple, time-saving, solvent free	multiple cycles required for desired particle size, small sample particles needed	(Chen *et al.*, 2011; Hecq *et al.*, 2005; Keck and Müller, 2006; Patravale *et al.*, 2004)
Bottom up techniques			
Precipitation/Crystallization	simple, low cost	uncontrollable crystal growth during precipitation, drug must be soluble at least in one solvent, rapid crystal growth can result in crystal imperfection and inclusion of impurities	(Müller *et al.*, 2000; Rabinow, 2004)
Spray drying	narrow size distribution,	thermal stress, drug should be	(Broadhead *et al.*, 1992; Liu *et*

	yields spherical particles, one-step method	soluble at least in one solvent, costs of the method	*al.*, 2015b; Patel *et al.*, 2015)

The term micronization refers to procedures in which particle size is reduced to a few micrometers, usually to 1-10 μm (Bansal *et al.*, 2011). Micronization itself facilitates drug dissolution, but it is not considered as a suitable way for solubility enhancement. Therefore much more interest has been given to the preparation of nanosized particles or nanosuspensions.

One of the major drawbacks of particle size reduction arises from the increase of surface area and of surface energy resulting in a greater tendency to agglomerate. Thus the control of surface particles can be vital. Moreover, crystal imperfections, and formation of amorphous regions can decrease stability, as well (Shoyele and Cawthorne, 2006). On the other hand, declined flow properties and wettability may constitute barriers to further processing, *e.g.* tableting (Karavas *et al.*, 2006).

3.2.2. Amorphous solid dispersions

Preparation of amorphous solid drug dispersions (ASDs) offers a promising means of increasing solubility. ASDs are multicomponent systems comprising an amorphous active ingredient in a carrier, that is usually a polymer (Newman *et al.*, 2015). In ASDs, the active ingredient forms amorphous clusters in the carrier (Fig. 4). The principle of this method is the circumvention of low thermodynamic aqueous solubility by means of development of a solid system containing poorly soluble drug in a metastable state possessing an apparent solubility greater than that of the initial drug. ASDs are often referred to as spring-parachute systems. By virtue of their high chemical potential, drugs incorporated in ASDs are spouted in the dissolution fluid resembling a compressed spring. However, this higher energy form of the drug tends to precipitate, but the applied excipients act like a parachutes by hindering precipitation (Guzmán *et al.*, 2007) .

It is considered that the decisive energy among three quantities given in Eq. (1) is $E_{Crystal\ Packing}$, that is greater than the other two values. For this reason any efforts done to decrease $E_{Crystal\ Packing}$ engenders in a notable solubility improvement (Brough and Williams Iii,

2013; Lipinski *et al.*, 2012). Basically, in the course of getting contact with gastrointestinal fluids, ASD releases its active ingredient forming a thermodynamically unstable supersaturated solution (a solution in which a solute has a concentration greater than its equilibrium concentration) (Brouwers *et al.*, 2009).

Because of their numerous benefits, such as enhanced wettability, higher porosity and increased specific surface area, ASDs have gained particular interest in new formulation strategies (Karavas *et al.*, 2006). As a result of the presence of the polymeric matrix, ASDs exhibit better physicochemical stability than neat amorphous actives themselves. This can be attributed to the decreased molecular mobility originating from drug-excipient interactions (Taylor and Zografi, 1997; Yoshioka *et al.*, 1994; Zhou *et al.*, 2007). Molecular mobility has an impact on phase separation and drug recrystallization, therefore it is crucial from the point of stability (Janssens and Van den Mooter, 2009). Formation of strong drug-polymer interactions (ionic interactions and hydrogen bonds) and polymer-drug miscibility are of special impact for the physical stability (Li *et al.*, 2014; Tian *et al.*, 2014). In addition, polymers and surfactants hamper drug recrystallization during dissolution through the solubilization of the active. Another important aspect of ASDs relates to the wide range of polymers enabling the achievement of modified release.

On the contrary, the miscibility of the active and polymer is limited, therefore high weight fraction of the drug can lead to phase separation (Qi *et al.*, 2010; Six *et al.*, 2002; Six *et al.*, 2004). Thus along with poor physical stability, the limited drug loading capacity can be considered one of the major disadvantages of this approach.

Preparation of ASDs can be carried out using a solvent, a melting or a solvent-melting method, as well (Brough and Williams Iii, 2013; Squillante and Sethia, 2003). Solvent methods are based on the evaporation of a solvent from the solution of the drug and the polymer. Melting techniques require for the heating of the drug-excipient mixture above its glass transition temperature, and then for a cooling step with due regard to avoid recrystallization. The most frequently applied methods are listed in Table 2.

Table 2 Overview of the solvent and melting techniques

Method	**Advantages**	**Disadvantages**	**References**
Melting methods			
Hot-melt extrusion	modified release, reduced number of processing steps, uniform drug distribution, continuous process, high throughput rate, solvent-free	thermals stress, recrystallization upon cooling, high energy input, shear forces	(Breitenbach, 2002; Crowley *et al.*, 2007; Repka *et al.*, 2007)
Injection molding	solvent-free, continuous process, rapid technique, scalability and patentability, possibility of autosterilization	high pressure, high temperature	(Konig *et al.*, 1997; Zema *et al.*, 2012)
Solvent methods			
Spray drying	narrow size distribution, yields spherical particles, one-step method,	thermal stress, drug should be soluble at least in one solvent, costly, toxicity of organic solvents	(Broadhead *et al.*, 1992; Liu *et al.*, 2015b; Patel *et al.*, 2015; Weuts *et al.*, 2004)
Lyophilisation	aqueous and organic solutions, high porosity,	costly, requires a great amount of water to dissolve poorly soluble drug, toxicity of organic solvents	(Ahmed *et al.*, 2006; El-Badry and Fathy, 2006; Oetjen and Haseley, 2007)

3.2.3. Solid solutions

Solid solutions (SSs) are solutions comprising a solid solute in a solid solvent, hence the solute is molecularly dispersed resulting in the formation of a homogenous amorphous phase (Fig. 4). Glass solutions should be also noted here, where a solid is dissolved in glassy system, but in the relevant literature there is no consensus for the differentiation of these terms, they are often referred as synonyms (Chiou and Riegelman, 1971; Patterson *et al.*, 2007). In general, the formulation of SSs result in a transparent system, while ASDs are usually opaque. It is not an effortless attempt to uncover the differences by using traditional physicochemical methods, *e.g.* differential scanning calorimetry (DSC), powder X-ray diffraction, Raman spectroscopy or Fourier transform infrared spectroscopy (FTIR), since the results of such measurements usually do not indicate the nature of the system. Nevertheless, modern techniques, such as solid-state nuclear magnetic resonance provide opportunity to gain information about the nature of the dispersion characteristics of the drug (Djuric *et al.*, 2010; Ito *et al.*, 2010; Pham *et al.*, 2010; Stejskal *et al.*, 1981).

The theoretical background of the solubility and dissolution enhancement effect of SSs is the same as expounded in the previous section above. The main difference lies in the distribution of the incorporated drug. By reason of the molecular dispersion, SSs represent the pinnacle of the amorphous formulations, since this approach takes advantage of particle size reduction and amorphous conversion as much as possible. In view of reduced molecular mobility and molecular dispersity, the statistical probability of encounter of drug molecules to form crystals is much lower than in other systems.

Basically, all of the techniques listed in Table 2 are capable for the formulation of SSs suggesting that the formation of SSs or ASDs depends on the applied excipients and process parameters rather than the chosen method. It has been found that the development of strong drug-excipient interaction plays a pivotal role from the point of the formation of SSs (Aldén *et al.*, 1993). On the other hand ensuring good miscibility is also essential (Andrews *et al.*, 2010).

Polymeric micro- and nanofibers represent unique carrier systems, that are also capable for the formulation of SSs and they are discussed in details in the next section.

3.3. Polymeric micro- and nanofibers in the pharmaceutical research

Even though, naturally occurring fibrous systems have been long present in the human history (such as cobweb, plant fibers or musculoskeletal tissues) the consideration of these structures as potential drug delivery systems is quite a new concept. Nowadays, the role of polymeric fibers in the formulation development of special dosage forms is unquestionable, which is well supported by the growing interest for these systems. Fig. 5 strikingly demonstrating that over the past 20 years the number of documents published concerning this topic have been sharply increased.

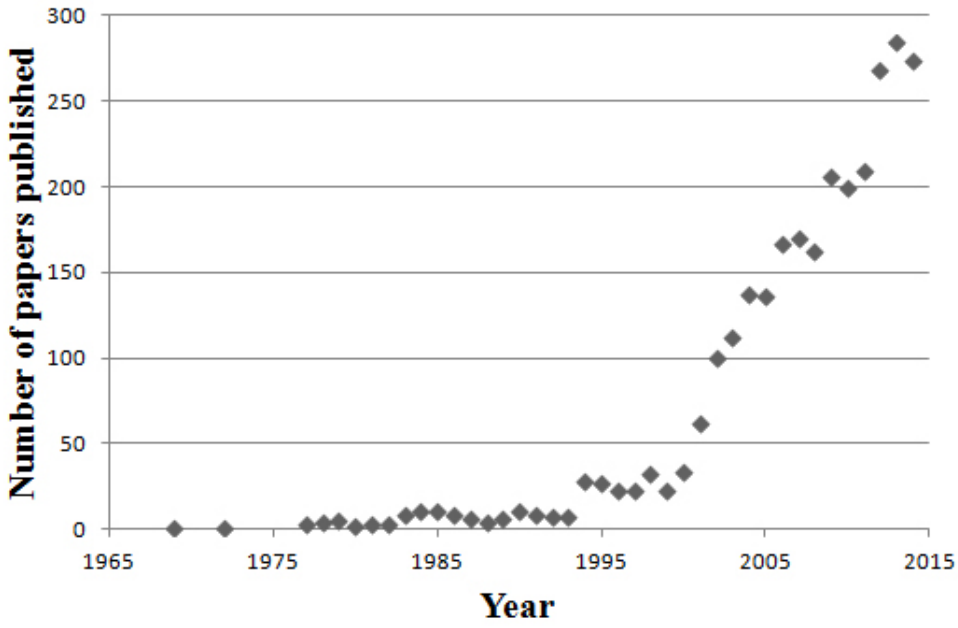

Figure 5 Number of published documents per year based extracted from Scopus search results analysis using the following keywords: fiber, drug delivery system

3.3.1. Structure and physicochemical features of polymeric fibers

Polymeric fibers owe their popularity to their unique physicochemical characteristics, which are well exploitable for the formulation of innovative drug delivery systems.
Because of their fibrous nature and small diameter, they can be characterized with high specific area-to-volume ratio (Tennent *et al.*, 2000; Zhang *et al.*, 2005b). High specific area-to-volume ratio is beneficial from the point of dissolution, since larger the surface area, the faster the drug dissolution, according to Eq. (2). High porosity and the possibility

to keep drugs in amorphous state are also a favorable properties for dissolution enhancement and for biological applications (Frenot and Chronakis, 2003; Szabó and Zelkó, 2015).

Since the structure of these fibers resembles to the extracellular matrix (ECM), these are potential candidates for tissue engineering applications. ECM has an important role in the regulation and maintenance of biologic function of living tissues through providing mechanical support and through the mediation of biological signals (Hay, 2013; Reddi, 2000). Fibrous scaffolds serve as an interim ECM until the regeneration and the formation of a native ECM.

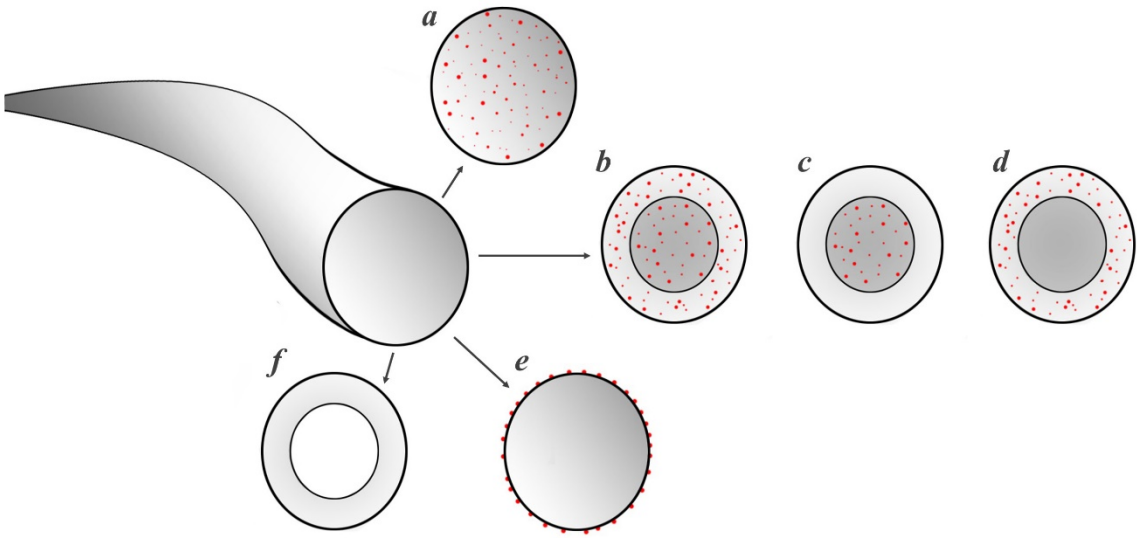

Figure 6 Basic types of polymeric microfibers, *a*: blend type, *b-d*: core-shell type, *e*: immobilized, *f*: hollow fibers

Furthermore, the availability of natural polymers, such as collagen makes these systems even more attractive for biological applications, since the more perfectly is the mimicking, the better repairing efficacy can be achieved (Pham *et al.*, 2006).

As can be seen from Fig. 6, different types of fibers can be classified based on the distribution of the drug and the applied polymers.

Blend or matrix type fibers represent a simple structure consisting a drug uniformly dispersed in a carrier matrix. Immobilized fibers comprise a neat carrier and a drug attached to its surface by chemical or intermolecular bonds. Core-shell fibers are built up of two coaxial matrices, the drug can be incorporated in various arrangements as

illustrated in Fig. 6. Furthermore, the inner part of the fiber can consist of drug only. For the time being, hollow fibers have meager pharmaceutical importance (Li *et al.*, 2005).

The fiber structure offers an opportunity to tailor release properties. While in case of blend type fibers, the drug release depends on the hydrophilicity of the chosen polymer, in case of core-shell type fibers sustained release, and biphasic release can be also achieved (Jiang *et al.*, 2012; Szabó and Zelkó, 2015; Yu *et al.*, 2013).

Surface properties play a critical role in drug delivery and biological applications. Biocompatibility is usually a desired property, while biodegradability can be a supportive feature in certain cases (Pelipenko *et al.*, 2015). Beyond hydrophilicity or hydrophobicity, more broadly, surface properties cover the surface functionalization of fibers, too. Surface functionalization is the chemical modification or the coating of fibers (Fang *et al.*, 2008). Changing the chemical environment on the surface of fibers offers a tool for adjusting release properties, drug loading and surface hydrophobicity (Jacobs *et al.*, 2011; Xie *et al.*, 2012). For instance, developing ionic groups allows the formation of ionic interactions (Jiang *et al.*, 2014). Coating of fibers can aim at the preparation of stimuli-responsive drug delivery systems, such as pH-dependent drug dissolution or other release modifying purposes, *e.g.* reducing burst release (Jiang *et al.*, 2014; Risdian *et al.*, 2015; Zeng *et al.*, 2005a).

It has been demonstrated, that during the fiber formation, a supramolecular ordered structure can be developed (Cui *et al.*, 2006; Sebe *et al.*, 2013). The exact role of this kind of ordering in the function of fiber based formulations have been not revealed yet. But it can be proposed that this has an impact on molecular mobility and drug-excipient interactions, thus the stability of such formulations.

3.3.2. Polymers for fiber formation

Since the dawn of modern pharmaceutical development and manufacturing, polymers have received a particular attention, and this is no different for both micro- and nanofibers, where most of the relevant papers focuses on the formulation of polymeric based fibers. Accordingly, scientific publications cover the whole spectrum of polymers available. Basically, natural, semisynthetic and synthetic polymers are equally frequently used (Table 3).

Table 3 Polymers frequently applied in fiber formation classified by their origin

Source of polymer	**Representative**	**Reference**
Natural	sodium alginate	(Bonino *et al.*, 2011; Jeong *et al.*, 2010; Nie *et al.*, 2008)
	collagen	(Dong *et al.*, 2009; Liu *et al.*, 2010; Rho *et al.*, 2006; Song *et al.*, 2008)
	hyaluronic acid	(Ji *et al.*, 2006; Li *et al.*, 2006; Liu *et al.*, 2011; Um *et al.*, 2004)
	nucleic acids	(Fang and Reneker, 1997; Kim and Yoo, 2010; Liu *et al.*, 2007)
	cellulose	(Kim *et al.*, 2006; Kim *et al.*, 2005; Xu *et al.*, 2008)
Semisynthetic	chitosan	(Bhattarai *et al.*, 2005; Geng *et al.*, 2005; Ohkawa *et al.*, 2004)
	hydroxypropyl cellulose	(Shukla *et al.*, 2005; Szabó *et al.*, 2014a; Szabó *et al.*, 2014b; Szabó *et al.*, 2015)
Synthethic	poly(vinylpyrrolidone)	(Adeli, 2015; Sebe *et al.*, 2014; Sebe *et al.*, 2015; Sebe *et al.*, 2013; Vigh *et al.*, 2013)
	poly(vinyl alcohol)	(Kenawy *et al.*, 2007; Taepaiboon *et al.*, 2006; Zhang *et al.*, 2005a)
	poly(lactic acid)	(Liu *et al.*, 2015a; Monnier *et al.*, 2015; Sonseca *et al.*, 2012; Xu *et al.*, 2006)

	poly(glycolic acid)	(Boland *et al.*, 2001; Dong *et al.*, 2008; Hajiali *et al.*, 2011)
	poly(lactic-*co*-glycolic acid)	(Xie and Wang, 2006; You *et al.*, 2006)

The paramount functionality-related characteristics of the polymers are the solubility, wetting properties, biodegradability and biocompatibility.

Solubility of the polymer plays a decisive role during the formulation, because the solubility of the chosen polymer has a great impact on the release kinetics of the active substance. Generally, the use of water soluble, hydrophilic polymers results in a rapid, immediate drug release, while hydrophobic or swelling polymers could be exploited in controlled release formulations (Szabó and Zelkó, 2015). So-called release modifying agents are low molecular weight hydrophilic polymers or surfactants (*e.g.* poly(ethylene glycol)), which can enhance surface hydrophilicity, thus facilitating the proper drug dissolution (Maretschek *et al.*, 2008; Puhl *et al.*, 2014). Biodegradability, *i.e.* the hydrolytic or enzymatic degradation of the carrier is relevant in terms of erosion controlled drug delivery systems, as well as biological applications, where the role of fabricated fibrous scaffold will be replaced by the continuous generation of the ECM. The relevance of biocompatibility is mainly pronounced in biological applications, where the interaction of the living tissues and their constitutive cells is a key element of the biological effect.

3.3.3. Fiber formation techniques

In the scientific literature several methods are known for fiber formation, however the vast majority of the publications focuses on only a couple of techniques. Classification of these methods can be performed considering various aspects, such as the nature of the sample or the driving force of the fiber formation. Thus we can distinguish physical and chemical methods, but it should be noted that the former is much more dominant. The driving force of the physical fiber formation can be solvent evaporation or cooling supported by electrostatic, pneumatic or centrifugal forces. Table 4 summarizes the available methods for fiber preparation. The table also highlights the versatility of

electrospinning, forcespinning and blowspinning, since these techniques can handle either solutions or melts; hence these are the most favorable choices for pharmaceutical purposes. Furthermore, electrospinning process can be facilitated with air blowing (Nayak *et al.*, 2011).

Table 4 Fiber formation techniques (Nayak *et al.*, 2011)

Fiber formation method		
Chemical methods	*Physical methods*	
	Solvent based methods	*Melt methods*
interfacial polymerization	electrospinning	electrospinning
template synthesis	forcespinning	forcespinning
self-assembly	solution-blow spinning	melt-blow spinning
	drawing	template melt extrusion
	phase separation	

3.3.3.1. Electrospinning

Because of its easy configuration, versatility and scalability, electrospinning has emerged as the most popular technique for fiber formation. This technique provides a great control over product characteristics and enables the preparation of almost every kind of fiber structures. The principle of electrospinning is epitomized in Figure 7. This method requires for a viscoelastic sample; a solution or melt, which is put in a syringe with a needle on it and then it is exposed to a high voltage. When the applied voltage is large enough to overcome the surface tension, polymeric jets will be ejected. In more detail, the high voltage upsets the equilibrium between surface tension and electric field potential, which stabilizes the shape of a droplet. This disturbance leads to the conical deformation of the droplet developing the so-called Taylor cone (Fig. 7). The unstable state results in the fission of Taylor cone, thus jet formation can take place (Yarin *et al.*, 2001). The formed electrostatic field also expedite fiber production by accelerating and stretching jets towards the collector. The solidification of the ejected jets by the evaporation of solvent or cooling enables the formation of solid fibers (Pham *et al.*, 2006; Teo and Ramakrishna, 2006). Finally, fibers are caught on the surface of the grounded collector. Electrospinning produces continuous fibers of a diameter ranging from a few

nanometers to a few micrometers. Hitherto, more than 200 polymers have been reported to be suitable for electrospinning remarkably indicating its significance (Bhardwaj and Kundu, 2010).

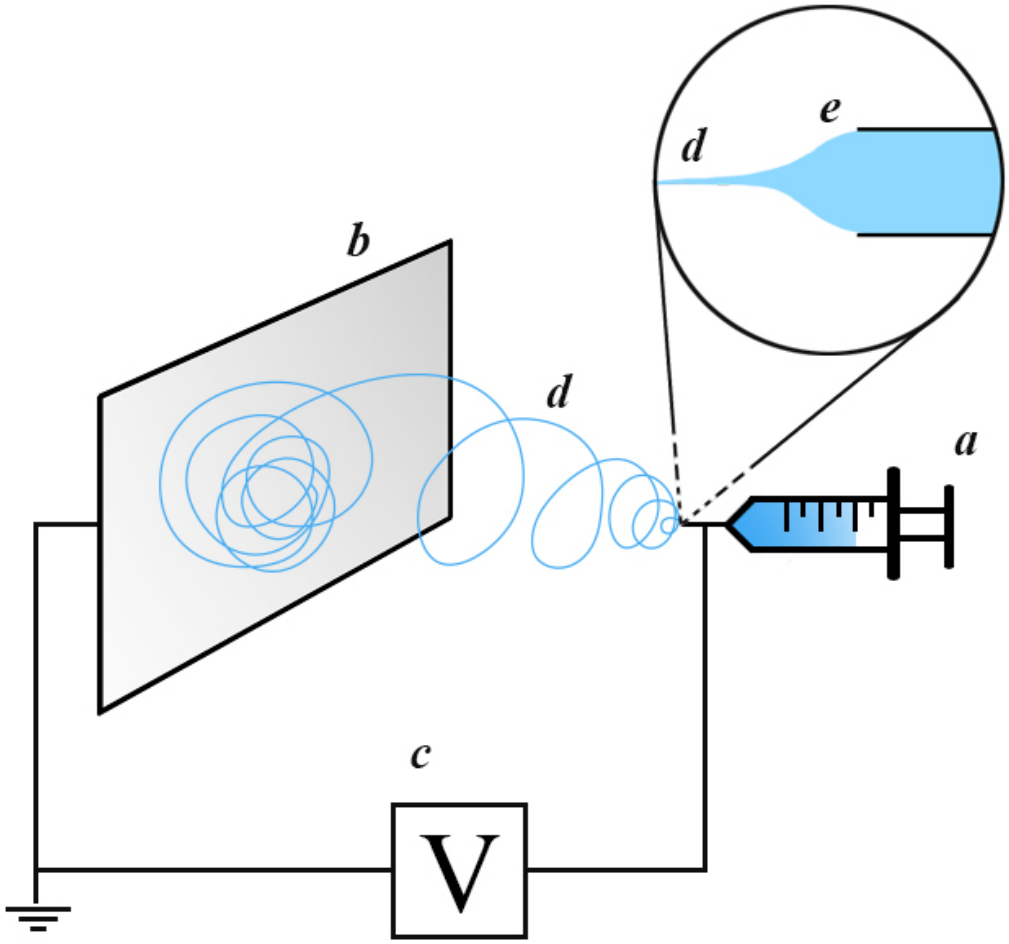

Figure 7 A schematic representation of a typical electrospinning arrangement, *a*: syringe equipped with a needle and filled with polymer solution or melt, *b*: collector, *c*: high voltage power supply, *d*: jet ejected from the needle, *e*: Taylor cone

Table 5 summarizes the critical parameters influencing fiber morphology including diameter and bead formation. These parameters can be classified as process, solution and ambient parameters.

Table 5 The most important factors influencing electrospinning (Pelipenko *et al.*, 2013)

Critical parameter		
Process parameter	*Solution parameter*	*Ambient parameter*
applied voltage	polymer molecular weight	temperature
flow rate	viscosity	humidity
needle-collector distance	surface tension	
needle construction	solvent, solvent mixture	
collector	conductivity	
	dielectric constant	

Beyond the basic arrangement displayed in Fig. 7, more complex apparatuses are available aiming at the preparation of special fiber structures or oriented fibers. The manufacturing of blend fibers is the more effortless, where drug and polymer are mixed together prior to the fiber formation. For the preparation of core-shell type fibers emulsion of two polymers or a specific coaxial electrospinning apparatus (equipped with a core-shell nozzle) is required (Yarin, 2011).

3.3.3.2. High speed rotary spinning

Forcespinning or high speed rotary spinning has been receiving an increasing attention for pharmaceutical applications. The fundamental of the method is depicted in Fig. 8.
In the course of this process, a viscoelastic polymeric solution or melt is put into a rotating reservoir, which has small wall orifices on its wall and is driven by a controlled engine. A revolution speed is achieved that is large enough to develop a centrifugal force capable to overcome capillary forces, thus the polymeric sample is pressed through the orifices. Finally, the lengthening jet will solidify upon solvent evaporation and rapid cooling. This method also produces continuous fibers. Beyond the driving force, one of the most important difference from electrospinning, that this method typically employs more concentrated polymeric solutions (Sarkar *et al.*, 2010; Szabó and Zelkó, 2015).

DOI:10.14753/SE.2016.1927

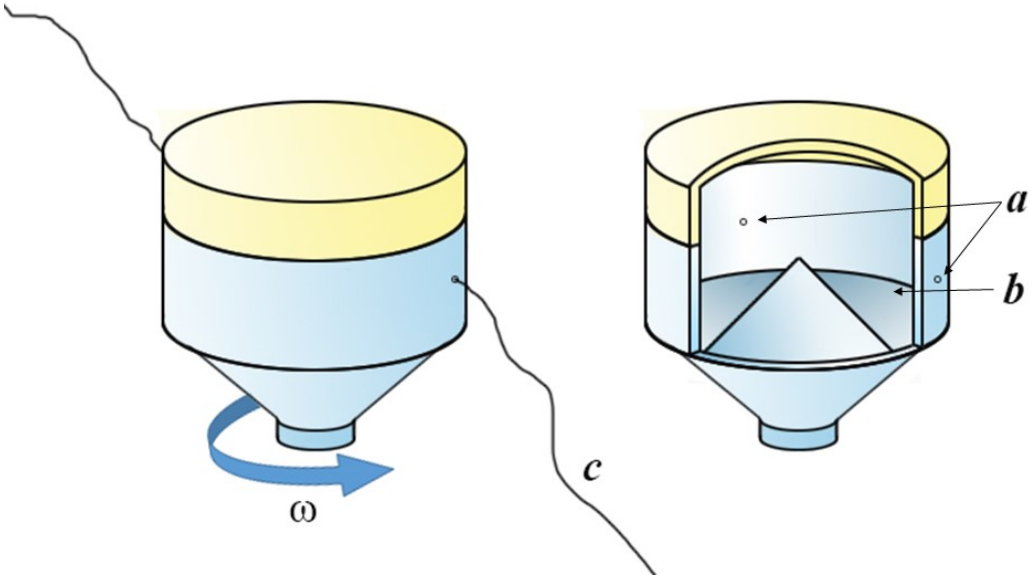

Figure 8 Schematic and cutaway drawing of a spinneret applied for high speed rotary spinning, *a*: wall orifices, *b*: rotating reservoir, *c*: ejected polymeric jet or fiber, *ω*: angular velocity

Angular velocity and radius of the rotating reservoir determines centrifugal force, according to

$$F_{cent} = m\omega^2 r \qquad (7)$$

where F_{cent} is the centrifugal force, *m*, ω and *r* represent the weight, angular velocity and radius of the rotating mass, respectively (Eq. (7)).

Table 5 The most important factors influencing high speed rotary spinning (Badrossamay *et al.*, 2010)

Critical parameter		
Process parameter	*Solution parameter*	*Ambient parameter*
angular velocity	polymer molecular weight	temperature
radius of reservoir	viscosity	humidity
diameter of orifice	surface tension	
	solvent, solvent mixture	
	volatility	

Fiber formation is in strong connection with the capillary number which is defined as

$$Ca = \frac{U\eta}{\gamma} \quad (8)$$

where *Ca* is the capillary number, η is the dynamic viscosity, γ is the surface tension and *U* is the polymer jet exit speed (Eq. (8)). It was found that above critical solution concentration (the concentration above which fiber formation take place) the higher the Ca, the better the quality of the prepared fibers and the smaller the tendency for bead formation (Badrossamay *et al.*, 2010).

3.3.4. Preparation of drug loaded micro- and nanofibers

Preparation of drug loaded micro- and nanofibers can be carried out in several ways. The loading of polymeric fibers can be direct and indirect. In case of direct loading drug containing polymeric solutions, suspensions or melts are applied during the fiber formation process. In respect of indirect or active loading, neat fibers are prepared prior to the introduction of the active ingredient.

The use of drug containing gels or solutions can be considered as the most convenient approach. However, this way of loading has some limitations:

- the applied drug must be soluble at least in one solvent;
- the applied solvent should be a good solvent for each component in order to avoid phase separation;
- blend type fibers usually suffers from burst release;
- potential harm of solvent residues and
- the physicochemical stability of amorphous drug (Thakur *et al.*, 2008; Zeng *et al.*, 2005b).

The possibility to use melts is also advantageous, because of the solvent-free nature of the process. Nonetheless, the method is limited to thermoplastic polymers and to heat stable drugs.

Drug suspensions can be also subjected to spinning processes, but it is not a mainstream way of preparation drug loaded fibers. The ability of tailoring drug release through the modification of crystal characteristics, the thermodynamically stable nature of crystals are the advantages of the use of crystalline drug suspensions (Müller and Ulrich, 2012; Puhl *et al.*, 2014). It must be noted, that in case of high speed rotary spinning, the formed centrifugal force is incompatible with drug suspensions, because of its sedimentation effect.

Active loading was invented in order to address the issue of low drug loading capacity. In the course of this method, neat fibers prepared prior to the loading step are immersed in a solution of the drug, of which solvent does not dissolve the fiber forming polymer. Finally, the solvent will be evaporated. This proves also known as the non-solvent evaporation method (Kataria *et al.*, 2014).

DOI:10.14753/SE.2016.1927

4. RESEARCH OBJECTIVES

The general aim of the thesis was to demonstrate the importance of fiber-based approaches in the formulation of poorly soluble drugs and at the same time to highlight the prosperous possibilities hidden in high speed rotary spinning. My intention was to provide a comprehensive overview of the progress of a fiber-based formulation. Thus the thesis and its underlying experiments cover a broad spectrum of pharmaceutical development from the preformulation to the stability testing, therefore my aspirations were as follows.

- Enrichment of the range of polymers capable for high speed rotary spinning, by selecting a pharmaceutical polymer, namely hydroxypropyl cellulose (HPC) for high speed rotary spinning that have not been reported to be rotary spun so far.
- Conducting preformulation studies with HPCs of different average molecular weights in order to establish critical and optimal concentrations for fiber formation. The investigation of the impact of textural-rheological properties on fiber characteristics.
- By means of the exploitation of HPC's versatile solubility features (soluble both in water and ethanol), the preparation of drug loaded microfibers incorporating actives selected from BCS class II.
- Physicochemical and supramolecular characterization of drug loaded microfibers with a particular attention to the crystalline-amorphous transition.
- Formulation of a solid oral dosage form, *i.e.* orodispersible tablets from processed drug loaded microfibers for the dissolution enhancement of incorporated actives and for highlighting the inherent possibilities of oral administration of fibers.
- To obtain information on physicochemical stability of drug loaded fibers using accelerated stability test.

DOI:10.14753/SE.2016.1927

5. MATERIALS AND METHODS

5.1. Materials

Klucel® EXF Pharm and ELF Pharm type HPCs were selected for fiber formation (Ashland, USA). The average molecular weights are 80.000 and 40.000 (based on size exclusion chromatography), respectively, and the moles of substitution is 3.8 for each polymer.

Purified water (Ph. Eur. 8.) and the hydroalcoholic mixture of ethanol (96% v/v, Reanal, Hungary) and purified water (mixed in 3:1 volume ratio) were applied as solvents for the preparation of gels.

Pharmaceutical grade model drug (MD) for fiber preparation was selected from BCS class II, and can be defined with the following physicochemical properties: Mw < 500, pKa = 7.1 (with one basic centre), water solubility < 5.1 μg/ml, logP: 4–5.

The other pharmaceutically active ingredient was carvedilol (CD) (EGIS Pharmaceuticals Plc, Hungary, Ph. Eur.)

Citric acid monohydrate (Hungaropharma) was used for the preparation of drug stock solutions.

Concentrated hydrochloric acid (Molar Chemicals, Hungary), potassium dihydrogen phosphate (Molar Chemicals, Hungary), sodium hydroxide (Molar Chemicals, Hungary), and distilled water were applied in the preparation of the dissolution media.

The excipients of the orally disintegrating tablets were as follows: microcrystalline cellulose (Vivapur® 102 MCC) as filler and disintegrant, mannitol (Mannogem® EZ, SPI Pharma) or spray-dried lactose monohydrate (Flowlac®100, Meggle GmbH, Wasserburg, Germany) as filler, milled poly(ethylene glycol) 1500 (Macrogol 1500, Hungaropharma) or magnesium stearate (Ph.Eur. Hungaropharma, Hungary) as lubricant, equimolar mixture of milled citric acid anhydrate (Molar Chemicals, Hungary), and sodium bicarbonate (Hungaropharma) as effervescent agent and croscarmellose sodium (Vivasol®, JRS Pharma) as superdisintegrant agent.

5.2.1. Hydroxypropyl cellulose

Hydroxypropyl cellulose is a semisynthetic derivative of cellulose, a naturally occurring polymer. The polymer is official in different pharmacopoeias (e.g. European Pharmacopoeia, United States Pharmacopoeia) and widely applied for pharmaceutical purposes in oral and in topical dosage forms, as well. Chemical structure of HPC is illustrated in Fig. 9.

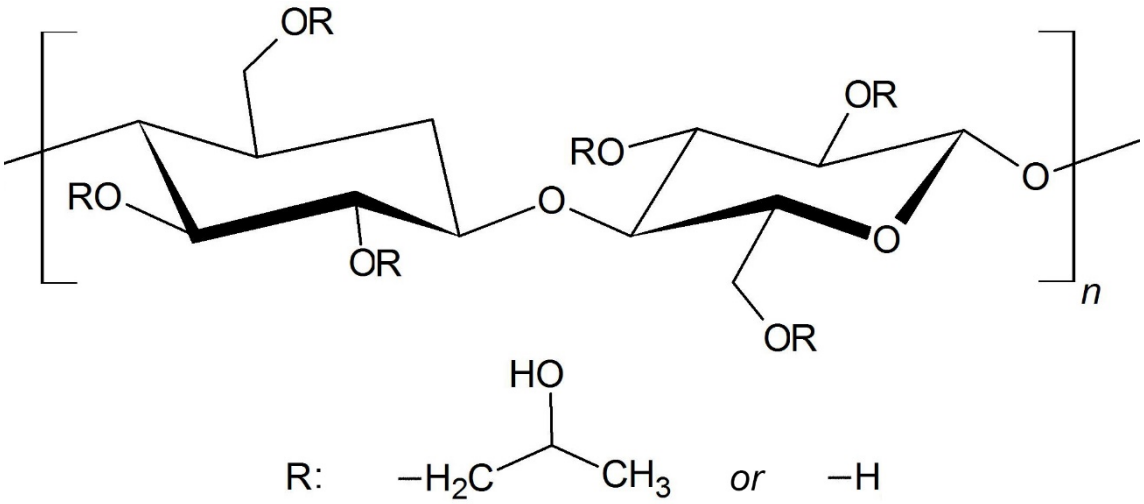

Figure 9 Chemical structure of hydroxypropyl cellulose

In pharmaceutical technology, HPC is mainly used as tablet binder, film coating agent and extended release matrix former (Rowe *et al.*, 2009). The polymer is freely soluble in water (below 38 °C) and in polar organic solvents, such as ethanol, dioxane, propanol.

5.2.2. Carvedilol

CD is an arylethanolamine type nonselective beta and alpha-1 adrenoreceptor blocker, which is used in the treatment of hypertension, coronary artery disease and congestive heart failure (Frishman, 1998; Morgan, 1994; Packer *et al.*, 1996; Ruffolo and Feuerstein, 1997). Chemical structure of CD is represented in Figure 10.

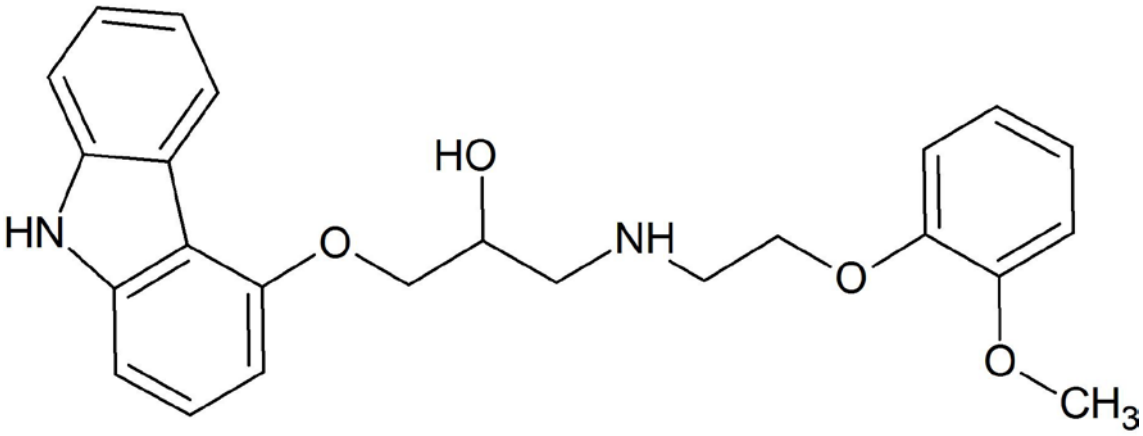

Figure 10 Molecular structure of carvedilol

CD exhibits poor aqueous solubility (27.11 ± 1.14 µg/mL in pH 6.8 buffer) and has a low oral bioavailability (below 25%), therefore it is a typical representative of BCS class II (v. Möllendorff *et al.*, 1987; Zhao *et al.*, 2011).

5.2. Sample preparations

5.2.1. Preparation of aqueous HPC gels

Aqueous gels were prepared in a beaker by the addition of water to HPC with due regard to their careful homogenization. Klucel® EXF gels were prepared in the concentration range of 38-52 % w/w, and Klucel® ELF gels were made in the concentration range of 42-60 % w/w with an increment of 2% w/w. In case of the former, gels were stored for 2 hours, in case of the latter, gels were stored for 1 hour at room temperature (T=25 °C) in order to ensure the complete dissolution of the polymers.

5.2.2. Preparation of drug containing HPC gels

For MD containing gels, the drug stock solution was prepared as follows. In a 50.00 ml volumetric flask, 5.000 g of drug was suspended with about the half of the necessary amount of hydroalcoholic mixture, until a lactescent dispersion was formed. Then 3.000 g of citric acid monohydrate (equimolar to drug) was added, and the dispersion was

shaken until a clear solution was formed. Finally, the solution was diluted to 50.00 ml with the solvent mixture.

For CD containing gels, the drug stock solution was prepared by the following way. In a 50.00 ml volumetric flask, 5.000 g of drug was suspended with about the half of the necessary amount of hydroalcoholic mixture, until a lactescent dispersion was formed. Then 2.590 g of citric acid monohydrate (equimolar to drug) was added, and the dispersion was shaken until a clear solution was formed. Finally, the solution was diluted to 50.00 ml with the solvent mixture.

Drug loaded gels of 50 % w/w Klucel® ELF were prepared by the addition of the equal amount of drug stock solution to the amount of polymer in a beaker. After careful homogenization and covering with paraffin tape, the gels were let to rest at room temperature (T=25 °C) for 1 hour.

5.2.3. Fiber formation

HPC fibers were prepared via high speed rotary spinning technique. At first, the samples were put in a perforated aluminum rotating reservoir, which was powered by a WSE 602 M engine (AEG, Germany). The fiber formation was carried out at 10,500 rpm. The rotational speed was controlled with a toroidal transformer and determined with laser revolution counter (DT-10L, Voltcraft, Germany). The internal diameter of the two wall orifices were 0.5 mm.

5.2.4. Preparation of physical mixtures

Following analytical assay of the drug loaded microfibers, physical mixtures of the same composition were made by the combination of plain drug, Klucel® ELF and citric acid. After sieving all components through a mesh sieve (nominal wire diameter 320 μm), the substances were homogenized in a Turbula (T2F model; Willey A Bachofen AG, Maschinenfabrik, Basel, Switzerland) at 23 rpm for 30 min in a cylindrical container. The mixture was used as control for the performed examinations, and for the preparation of control tablets.

5.2.5. Preparation of orodispersible tablets

Orodispersible tablets containing 10 mg drug were prepared by direct compression technique using a single-punch tableting machine (Diaf TM20, Copenhagen, Denmark), with a shallow concave round punch of 13.5 mm. Formulas are given in Table 6, where microfiber based tablets were assigned as TF, and control tablets consisting physical mixture of hydroxypropyl cellulose, anhydrous citric acid and drug were assigned as TPM. After sieving all components through a mesh sieve (nominal wire diameter 320 µm), the substances were homogenized in a Turbula (T2F model; Willey A Bachofen AG, Maschinenfabrik, Basel, Switzerland) at 23 rpm for 30 min in a cylindrical container. The batch size of 100 tablets was prepared for each composition and the tableting machine was powered manually.

To ensure specified hardness (30-35 N for MD and 40-45 N for CD containing tablets) the applied pressures were adjusted for each formula. Final weight of MD and CD containing tablets was adjusted to 500 and 600 mg, respectively.

Table 6 Composition of the prepared orodispersible tablets *Equimolar mixture of milled citric acid anhydrate and sodium bicarbonate

	Formulation series			
Component (% w/w)	**MD-TF**	**MD-TPM**	**CD-TF**	**CD-TPM**
Milled drug loaded microfiber (MD/CD)	20	-	11.10	-
Vivapur® 102	28	28	30	30
Milled poly(ethylene glycol) 1500	2	2	-	-
Magnesium stearate	-	-	1	1
Vivasol®	3	3	3	3
*Effervescent agent**	7	7	5	5
Mannogem® EZ	40	40	-	-
FlowLac®	-	-	49.90	49.90
Klucel® ELF	-	16.92	-	9.58
Crystalline drug (MD/CD)	-	2	-	1
Citric acid monohydrate	-	1.08	-	0.52

DOI:10.14753/SE.2016.1927

5.3. Measurements

5.3.1. Texture analysis

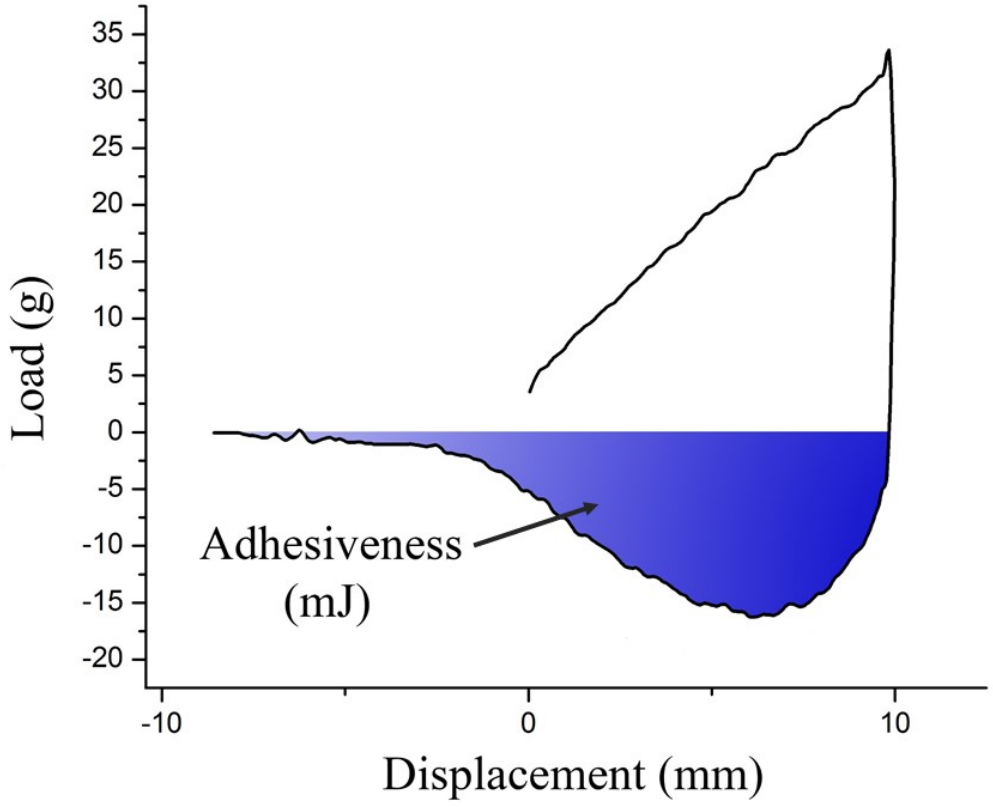

Figure 11 Calculation of adhesiveness from the load-displacement curve

Textural measurements were carried out using Brookfield CT3 Texture Analyzer with 4500 g load cell (Brookfield Engineering Laboratories, INC., USA) equipped with a cylindrical probe (TA-5, black delrin, diameter: 12.7 mm, length: 35 mm).

The compression test comprised two cycles applying the following parameters: pretest speed, test speed, and return speed of 2, 1 and 1 mm/s, respectively. Trigger load was set to 2 g. The probe compressed the gels through a depth of 10 mm as a target distance upon reaching the trigger load. Brookfield Texture Pro CT software was employed for evaluation. The adhesiveness is given by the total negative area of the load-distance curve of the first cycle (Figure 11).

DOI:10.14753/SE.2016.1927

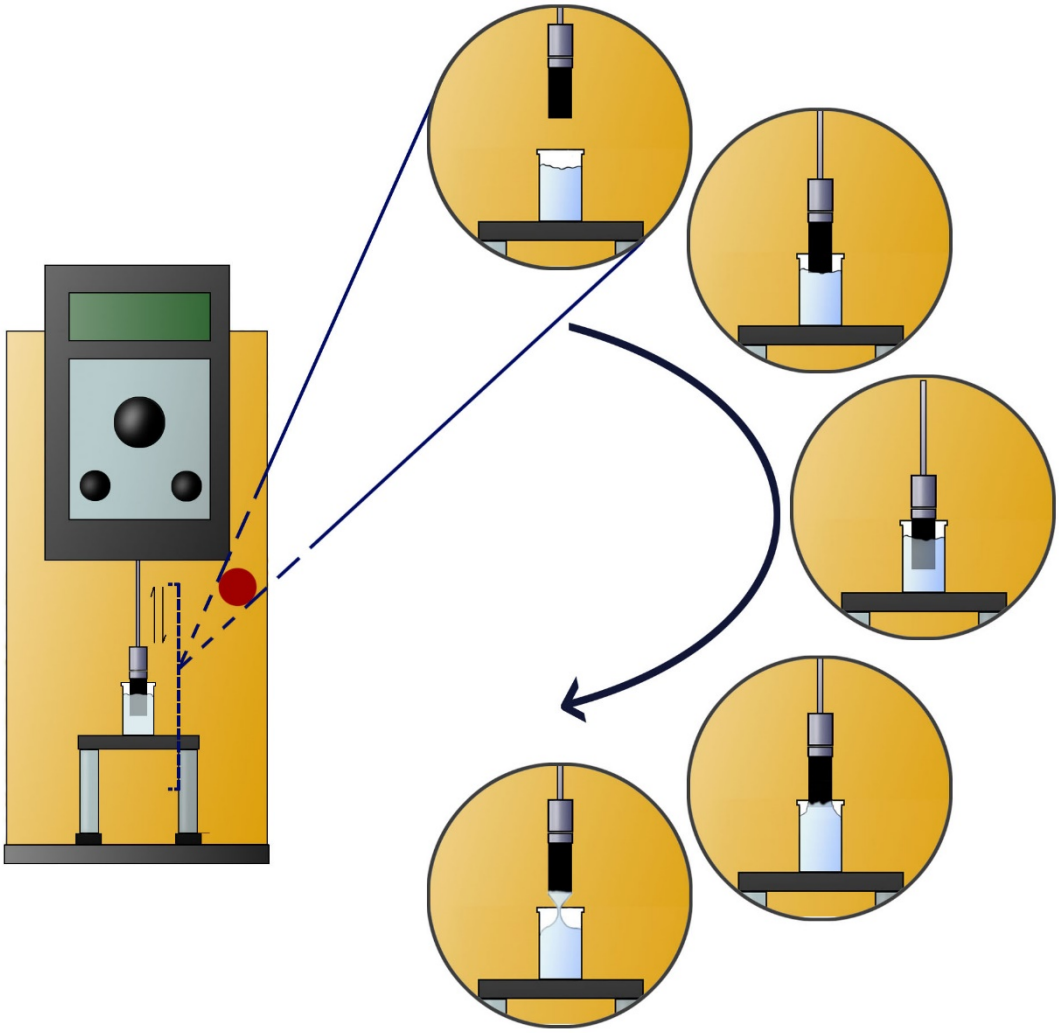

Figure 12 Measuring arrangement for adhesiveness determination with the motions of the probe

Prior to the measurement, 10.00 g of each sample was transferred to a cylindrical glass container (internal diameter: 23 mm, height: 30 mm), which was fixed to the platform of the instrument. Three parallels of each concentration were measured. The principles of the analysis is depicted in Figure 12.

5.3.2. Percentage yield

Percentage yield on dry polymer of the fiber formation process was calculated as follows (Eq. (9)):

$$Yield\ \% = \frac{m_{fiber}}{m_{gel}c_{polymer}}100 \quad (9)$$

where m_{fiber} is the weight of the fibers prepared from a gel of a weight of m_{gel} and a concenctration of $c_{polymer}$.

5.3.3. Morphological evaluation

Fiber morphology was characterized using both optical microscopes (LCD Micro type; Bresser; Germany and Nikon SMZ 1000 type; Nikon, Tokyo, Japan) and scanning electron microscope (SEM) (Amray 1830-D4,equipped with a tungsten electron gun and EDAX-PV 9800 energy-dispersive spectrometer). In the course of light microscopy magnifications were: 40x, 100x and a standard micrometer scale was used for the calibration. For SEM pictures, the parameters were as follows: acceleration voltage of 15 kV, beam current of 0.1–0.5 nA, and samples were gold coated with JEOL JEE-4B vacuum evaporator. Images were analyzed employing Image Pro Plus 4.5 software (Media Cybernetics, Bethesda, U.S.).

5.3.4. Milling process

Rotary knife grinder (Gorenje SMK 150 B) was applied for the particle size reduction of citric acid anhydrate, sodium bicarbonate, poly(ethylene glycol) 1500 and drug loaded microfibers. Operating parameters were as follows: milling time of 6 min, frequency of rotation was 24000 rpm (determined with DT-10L laser revolution counter, Voltcraft, Germany). All of the milled materials were sieved through a mesh sieve (nominal wire diameter: 320 μm).

5.3.5. Particle size characteristics

Information on particle size distribution was obtained by laser scattering particle size distribution measurement. The instrument (LA-950V2 Horiba Co., Kyoto, Japan) was equipped with a dry feeder unit to determine the particle diameter of the excipients and the milled drug loaded fibers in the range of 0.011-3000 μm. The operating parameters were as follows: air pressure of 0.1 MPa; feeder intensity (0-200) was 80; and relative refractive index was 1.60.

Distribution span values were calculated to characterize the width of the distributions based on Eq. (10):

$$Span = \frac{D_{90\%} - D_{10\%}}{D_{50\%}} \quad (10)$$

where $D_{10\%}$, $D_{50\%}$ and $D_{90\%}$ are the particle diameters at 10, 50 and 90% of the cumulative particles undersize plot. The results are the averages of five parallel measurements.

5.3.6. UV-Vis spectroscopy

Drug content of the milled fibers was measured by UV-vis spectroscopic assay (Agilent 8453 UV-Vis Diode Array System, USA for MD; and Jasco 530 UV–Vis spectrophotometer, Japan for CD) applying 0.1 M hydrochloric acid as solvent. The drug content of the samples was measured on the basis of the calibration curve recorded earlier. Five parallel measurements were performed.

5.3.7. Powder X-ray diffraction (XRD)

X'Pert Pro diffractometer (PANAnalytical, Almelo, The Netherlands) system with $CuK_{\alpha I}$ radiation (λ = 1.5406 Å) over the interval of 2.0000 - 40.0014° was used to obtain X-ray diffraction patterns. The following conditions were applied: target of Cu; filter of Ni (thickness was 0.02 mm); voltage of 40 kV; current of 40 mA; angular step of 0.0334°; counting time of 40.005 s.

5.3.8. Positron lifetime measurements

Supramolecular characterization of samples was carried out using positron annihilation lifetime spectroscopy (PALS). The method exploits the relatively long lifetime of the unstable exotic atom, ortho-positronium (o-Ps), which is formed after a positive beta decay upon bounding together with an electron. o-Ps atoms tend to be trapped in the free volume holes of polymeric excipients, and their annihilation is not influenced by their intrinsic lifetime but by the electron density in the holes. Deng et al. defined how o-Ps lifetime is associated with the size of the free volume around them (Eq. (11))

DOI:10.14753/SE.2016.1927

$$\tau_3 = \frac{1}{2}\left[1 - \frac{r}{r+\Delta r} + \frac{1}{2\pi}\sin\left(\frac{2\pi r}{r+\Delta r}\right)\right]^{-1} \quad (11)$$

where τ_3 is the ortho-positronium lifetime, r the radius of the free volume hole, and Δr is the electron layer thickness (Deng and Jean, 1993). According to Eq. 11, the longer the lifetime, the larger the hole.

For o-Ps determination carrier-free ^{22}NaCl positron source of an activity of 10^5-10^6 Bq was used with a fast-fast coincidence system based on BaF2 /XP2020Q detectors and Ortec® electronics. Three parallel spectra were measured at each composition to increase reliability. After summarizing the parallels, spectra were evaluated by the RESOLUTION computer code (Kirkegaard *et al.*, 1981); the indicated errors are the deviations of the lifetime parameters obtained. Three lifetime components were found in all the samples.

5.3.9. Differential scanning calorimetry

Thermograms of CD loaded microfibers were obtained using Seiko Exstar 6000/6200 (Seiko Instruments, Japan) differential scanning calorimeter with an open aluminum pan. The temperature range was 6°C - 200°C and the scanning rate was set to 5°C /min under air atmosphere. 0.0050 g of sample was used for the measurements.

5.3.10. Attenuated total reflectance - Fourier transform infrared (ATR-FTIR) spectroscopy examinations

ATR-FTIR spectra were collected on Jasco FT/IR-4200 spectrophotometer between 4000 and 2000 cm^{-1} with an ATRPRO470-H single reflection accessory (Jasco) equipped with flat pressure tip. The spectral measurements were performed in absorbance mode. The 200 scans at a resolution of 2 cm^{-1} were co-added by the FT-IR software (Spectra Manager-II, Jasco).

5.3.11. Tablet parameters

Hardness, friability and in vitro disintegration time were determined.

5 tablets of each composition were measured by tablet hardness tester (8M, Dr. Schleuniger Pharmatron, Switzerland).

For friability testing, ca. 6.5 g of dedusted tablets was put in an Erweka friability tester (TAP, Offenbach/Main, Germany). The instrument was moved for 4 min with a revolution speed of 25 rpm. Percentage friability was calculated by the reweighting of the dedusted tablets.

In vitro disintegration times were determined applying Erweka Disintegration Tester (ZT 4, Germany). 900 ml of demineralized water was used as the media; the measurement was carried out at 37±2 °C by visual observation (disk was not applied). Six tablets from each composition were evaluated for their disintegration times. The observed minimum and maximum values are reported later.

5.3.12. Dissolution test

Orodispersible tablets were examined in a Hanson SR8-Plus (Hanson Research, Chatsworth, USA) type dissolution tester equipped with rotating paddles at 37±1 °C, with a rotation speed of 50 rpm. Solution of hydrochloric acid of pH 1.0 (Ph. Eur. 8.), phosphate buffer of pH 4.5 (Ph. Eur. 8.) and phosphate buffer of pH 6.8 (Ph. Eur. 8.) were applied as dissolution media (the volume was 500 ml). 3.00 ml of samples were taken at predetermined time points using a Biohit Proline 5.00 ml pipette without refilling. The samples were filtered through a 10µm UHMW polyethylene cannula dissolution filter. The drug content of the samples was determined by UV-Vis spectroscopy (Agilent 8453 UV-Vis Diode Array System, USA for MD, and Jasco 530 UV–Vis spectrophotometer, Japan for CD) at the characteristic wavelength of the drug on the basis of the calibration curve recorded earlier. Three parallel measurements were carried out for each sample.

5.3.13. Comparison of the dissolution curves

Difference (f_1) and similarity (f_2) factors were calculated for the mathematical comparison of drug release profiles. Eqs. (12) and (13) were given by Moore and Flanner (Moore and Flanner, 1996) and implemented by FDA CDER (Center for Drug Evaluation and Research):

$$f_1 = \frac{\sum_{t=1}^{n'} |R_t - T_t|}{\sum_{t=1}^{n'} R_t} \times 100 \quad (12)$$

$$f_2 = 50 \times \log\left(\frac{100}{\sqrt{1 + \frac{\sum_{t=1}^{n'} (R_t - T_t)^2}{n'}}} \right) \quad (13)$$

where *n* is the number of time points, R_t is the dissolution value of the reference sample at time *t* (compressed physical mixture), and T_t is the dissolution value of the test sample (microfiber based formula) at time *t*. Two profiles can be considered to be similar if f_1 value is close to 0, and f_2 value is close to 100. Generally, f_1 greater than 15, and f_2 values smaller than 50 indicates significant difference between the dissolution of the test and reference product.

5.3.14. Accelerated stability study

Freshly prepared CD loaded microfibers were transferred into sealed snapcap vials. Afterwards, the samples were placed in stability chamber (Sanyo type 022, Leicestershire, UK) and maintained at 40 ± 2°C /75 ± 5% RH for 4 weeks. Samples subjected to stability test were analyzed by means of DSC, XRD, and ATR-FTIR spectroscopy and PALS.

DOI:10.14753/SE.2016.1927

6. RESULTS

6.1. Preformulation study

Aqueous HPC gels were simultaneously subjected to high speed rotary spinning and to texture analysis. The fiber formation was under optical microscopic monitoring.

Applying Klucel® EXF gels, fiber formation was successful between the concentration range of 46-50 % w/w, thus the critical minimum and maximum concentrations were 46 and 50 %w/w. Below the critical minimum concentration excessive bead formation took place, and above the critical maximum concentration no sample left the rotating reservoir under the given conditions. Figure 13 illustrate how changes of concentration influences morphology. The microscopic evaluation revealed that certain parts of fibers were helically twisted, and the phenomenon was observable at each concentration. The average fiber diameters are represented in Table 7.

Table 7 Average diameters of the prepared fibers

Concentration (% w/w)	**Mean diameter (µm) ± S.D.**	
	Klucel® EXF gels (n=50)	**Klucel® ELF gels (n=50)**
46	11.52±4.09	-
48	8.93±2.17	13.5±6.1
50	12.21±4.00	11.8±3.3
52	-	13.0±5.0
54	-	15.5±3.7

It can be seen, that the least fiber diameter was achieved when 48% w/w gel was applied, moreover the standard deviation was also the smallest.

Fig. 14 demonstrates the observed adhesiveness values and the percentage yield on dry polymer. The highest yield of fiber formation was obtained when applying 48% w/w gels. The shape of the adhesiveness curve is quite specific; at low concentrations the values are rising until they reach the peak, which is followed by a sharp decrease and ends in a plateau level.

These finding unanimously suggest that the optimal Klucel® EXF concentration for fiber formation is 48% w/w.

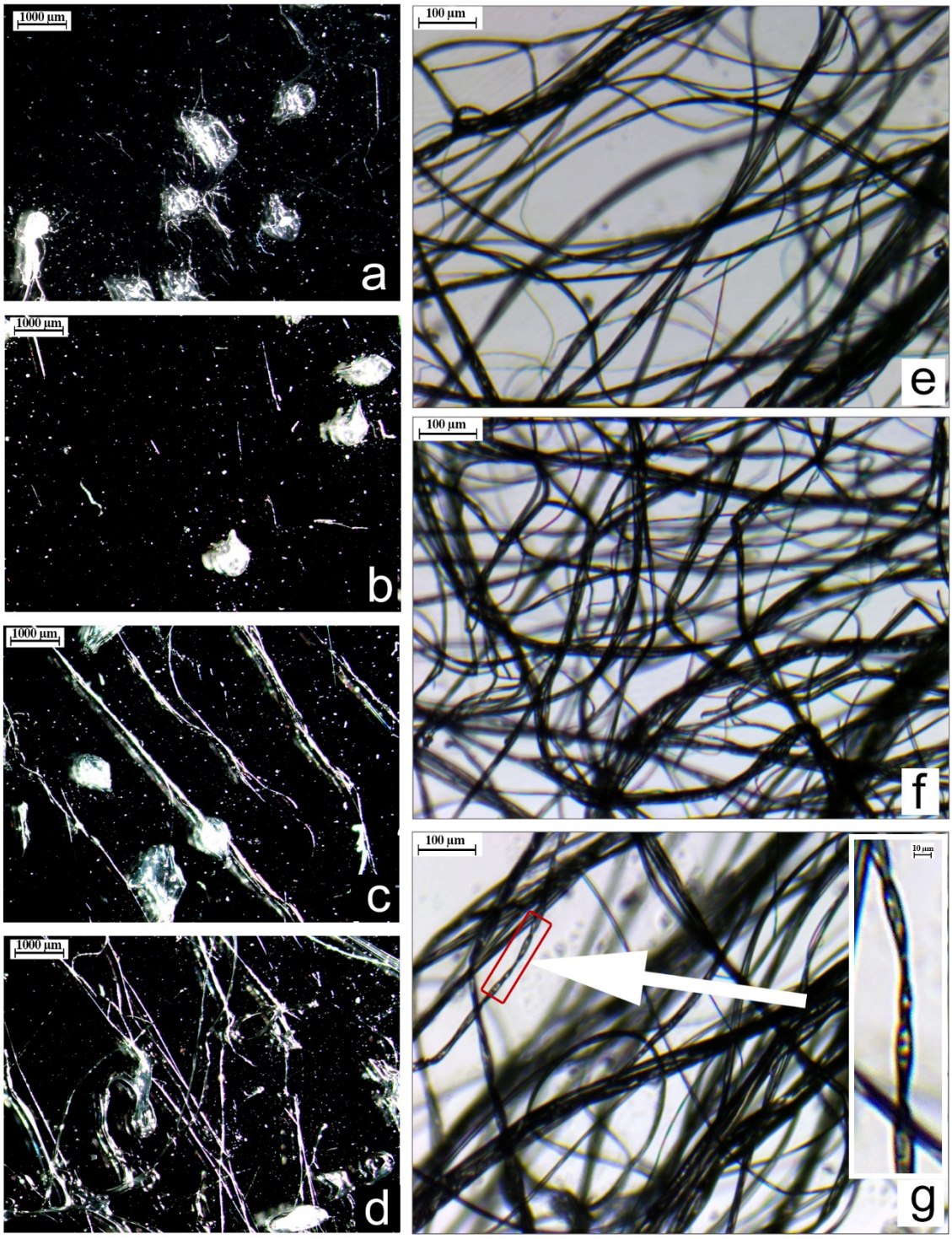

Figure 13 Optical microscopic morphology of fiber formation experiments using Klucel® EXF gels; *a:* 38; *b*: 40; *c:* 42; *d:* 44; *e:* 46; *f:* 48; *g:* 50 % w/w with a helical twisted region enlarged

DOI:10.14753/SE.2016.1927

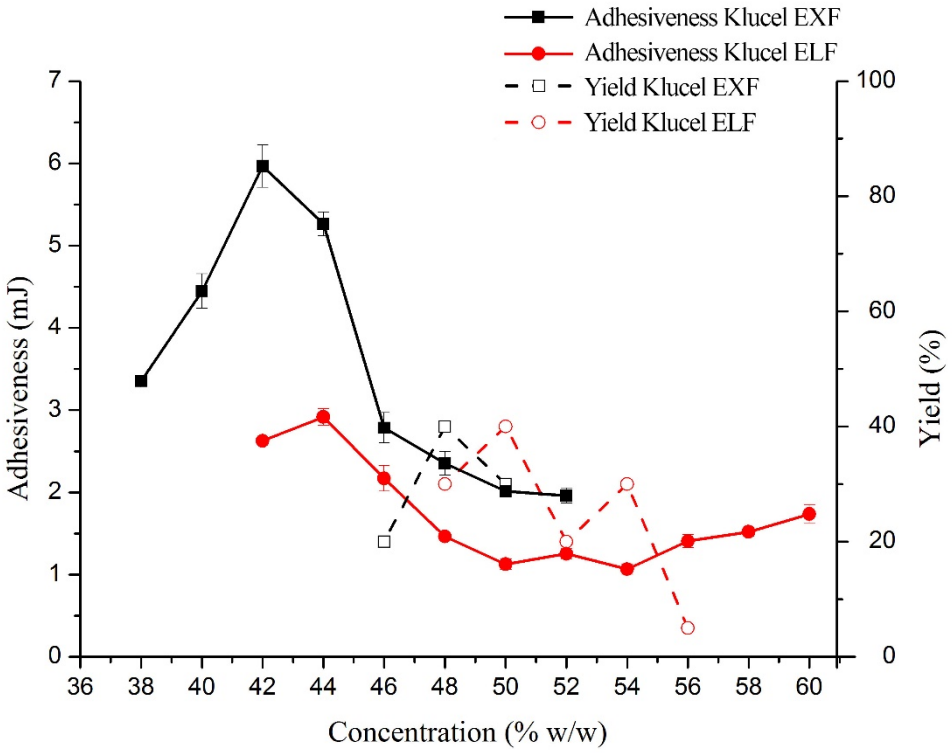

Figure 14 Adhesiveness values of aqueous HPC gels with the corresponding yields on dry substance

In case of gels made of Klucel® ELF, the critical minimum concentration was 48 % w/w, and the critical maximum concentration was 54% w/w. In respect of 42 % w/w gels, only droplets were formed, while in the concentration range of 42-46 % w/w bead formation was dominant over fiber formation. However, at above 54 % w/w, fiber formation took place, the fibers were too sticky, hence they were not capable for collecting and further processing. The morphology of the result of the fiber formation experiment can be seen in Fig. 15. Helically twisted regions were also found in the prepared fibers.

Average fiber diameters are listed in Table 6, in which the least diameter was obtained at 50% w/w. Similarly to the previous polymer, the smallest standard deviation was also related to the smallest fiber diameter. The highest yield of the process was obtained when 50% w/w gel was applied (Fig. 14).

The adhesiveness curve is partly similar to that of Klucel® EXF, but in addition to the maximum point, there can be found two local minimums (at 50 and 54% w/w).

DOI:10.14753/SE.2016.1927

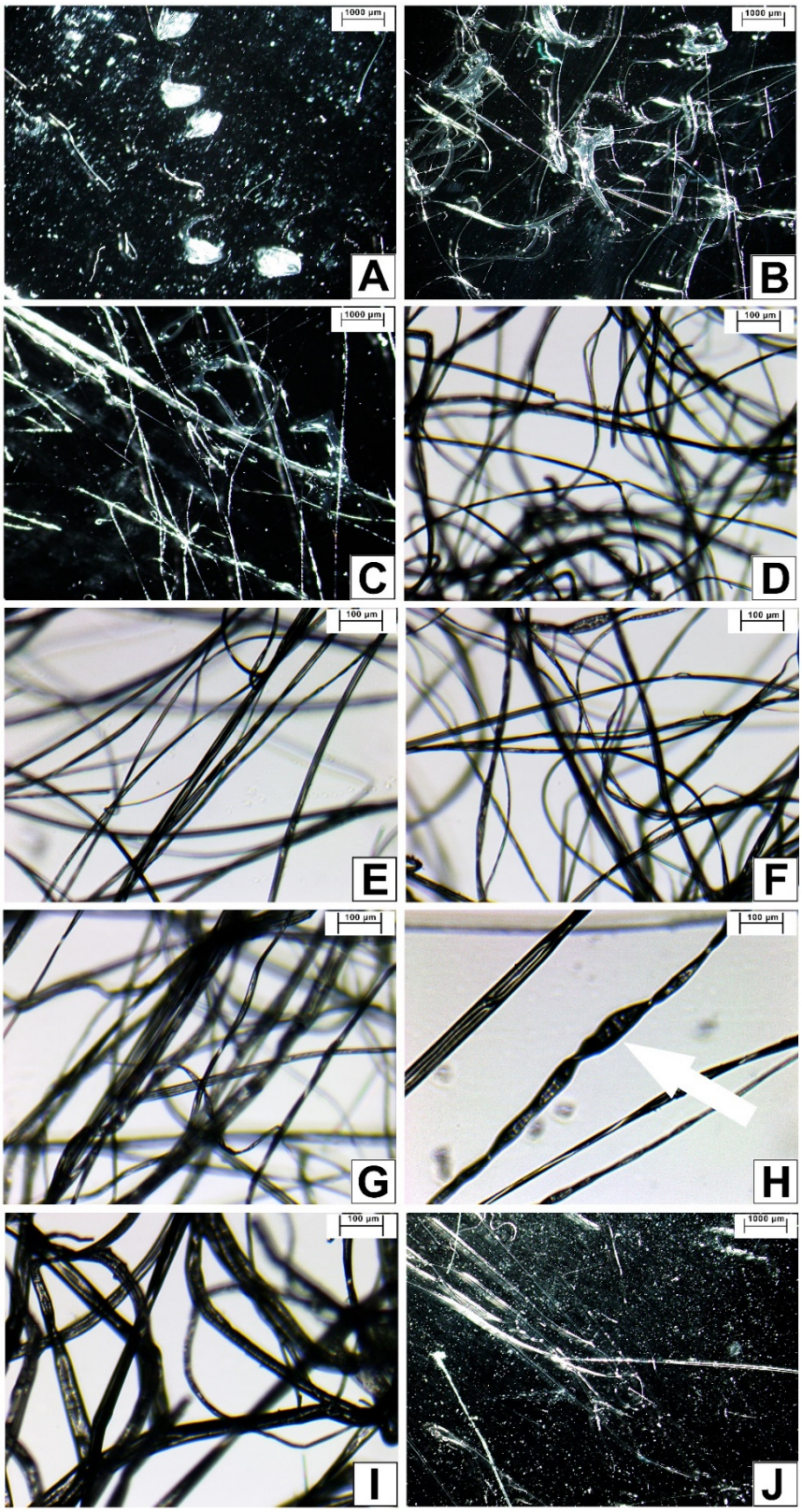

Figure 15 Optical microscopic morphology of fiber formation experiments using Klucel® ELF gels; *A:* 42 *B:* 44, *C:* 46, *D:* 48, *E:* 50, *F:* 52, *G:* 54, *H:* 56, *I:* 58, and *J:* 60 % w/w

Furthermore, instead of the plateau region, the adhesiveness values tend to rise again slightly above 54% w/w.

The performed examinations unanimously indicate that the optimal Klucel® ELF concentration for fiber formation with high speed rotary spinning is 50% w/w.

6.2. Preparation and investigation of drug loaded microfibers

Fiber formation via high speed rotary spinning was successfully carried out by the use of drug containing hydroalcoholic Klucel® ELF gels, of which previously determined optimal polymer concentration, i.e. 50% w/w was applied. Hereinafter, the two active ingredient will be expounded separately.

6.2.1. MD loaded fibers

Morphology of MD loaded fibers is displayed in Figure 16, indicating a clear, transparent fibrous structure with lack of observable beads. SEM pictures imply smooth surface of fibers, on which drug crystals are not detectable. Mean fiber diameter was given as 12.6±4.8 µm (n=50). The average drug content was 8.99±0.13% w/w (n=5).

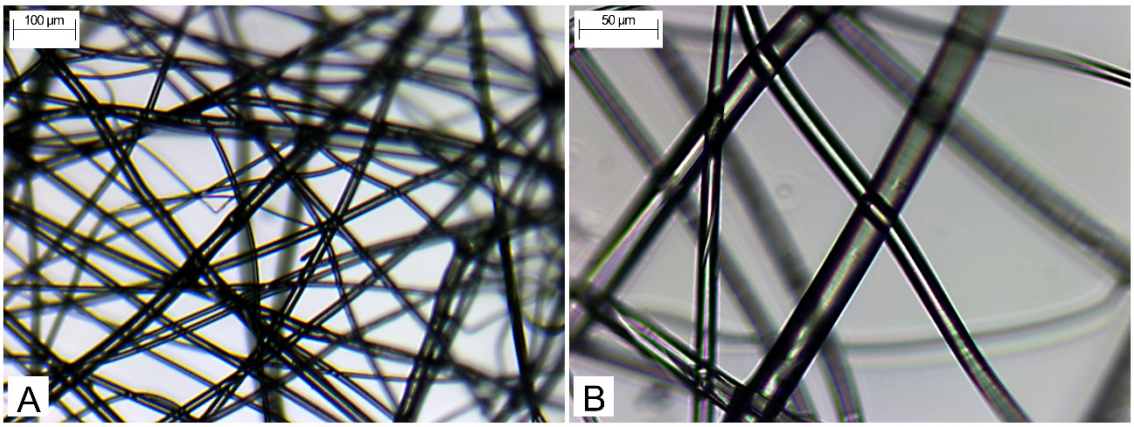

Figure 16 Optical microscopic appearance of MD loaded fibers, *A:* 40x, *B:* 100x magnification

X-ray diffractograms revealed a change in crystallinity of the active ingredient during fiber formation. In X-ray pattern of physical mixture, characteristic peaks of active ingredient are clearly detectable, combined with diffuse peaks of the amorphous polymer.

In respect of XRD pattern of the fibers, these characteristic peaks are not observable (Fig. 17). Long term ordering is a specific feature of crystalline materials, and as a result of this, X-rays are scattered in certain directions, which are characteristic to the substance. The absence of high intensity peaks implies the lack of the long term ordering, thus these findings indicate the crystalline amorphous transition of MD.

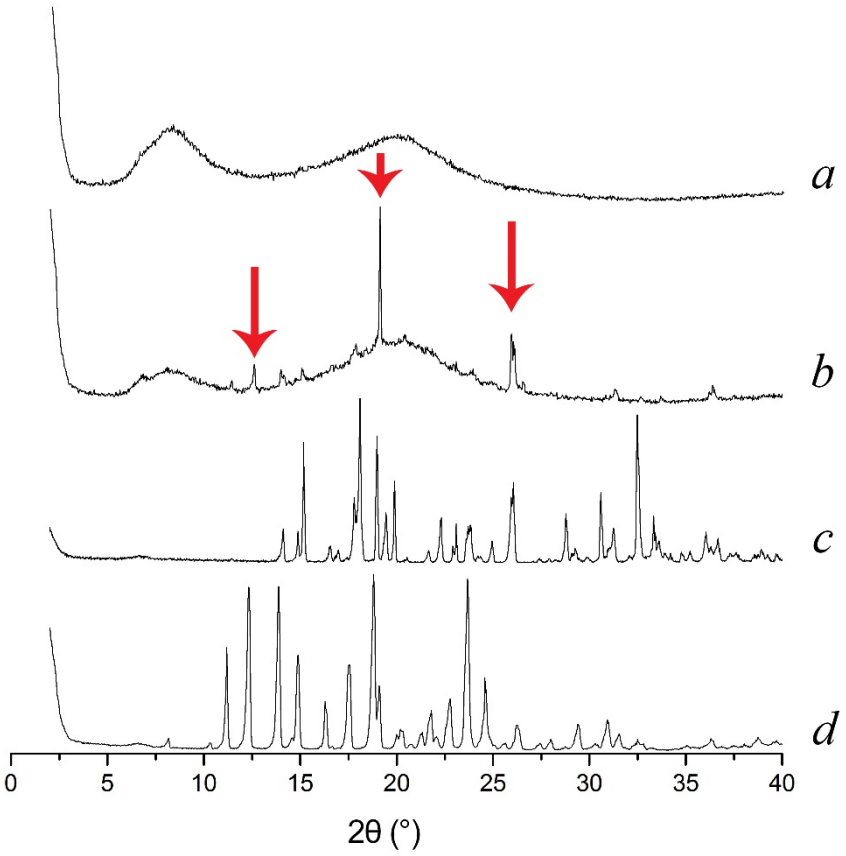

Figure 17 XRD patterns of the investigated samples, *a:* MD loaded microfibers, *b:* physical mixture, *c:* citric acid monohydrate, *d:* crystalline MD

PALS measurements also indicated a significant difference between fibers and the corresponding physical mixture. In case of the former, the decreased o-Ps lifetime, thus the reduction of free volume holes suggests the supramolecular ordering of the polymer chains (Fig. 18). It can be also associated with the formation of a SS, where amorphous drug is molecularly dispersed in the polymer matrix, which means that drug molecules wedged between the polymer chains reduce the size of free volumes. The transparent nature of the fibers also suggest this hypothesis (Fig. 16).

DOI:10.14753/SE.2016.1927

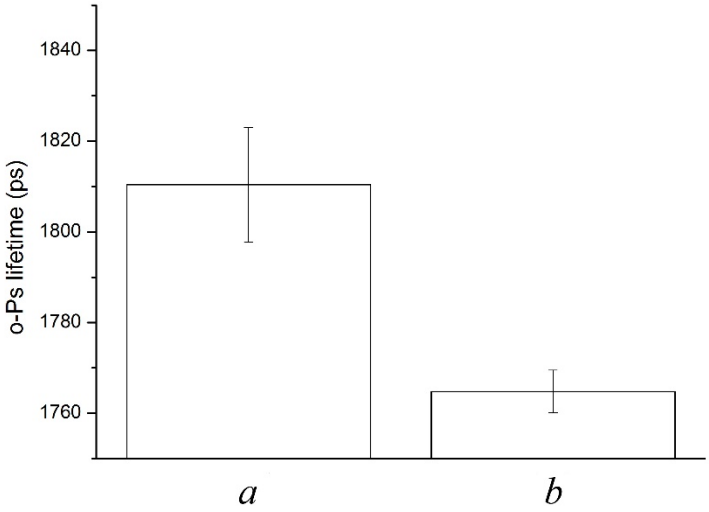

Figure 18 o-Ps lifetime values of investigated samples: *a*: physical mixture *b*: MD loaded microfibers

6.2.2. CD loaded microfibers

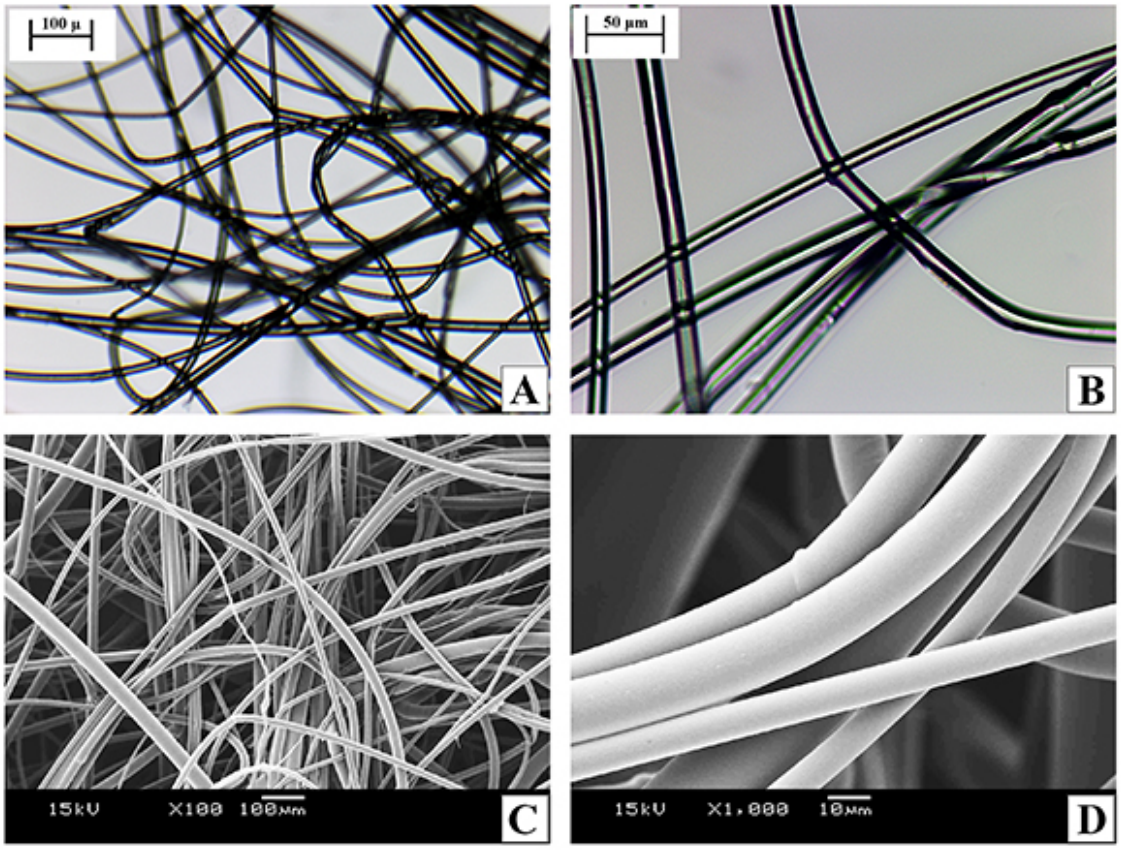

Figure 19 Micromorphology of CD loaded fibers: A and B: light microscopic record (40x and 100x magnification); C and D: SEM record (100x and 1000x magnification)

The microscopic morphology of fibers is represented in Fig. 19. Optical microscopic pictures reveal the formation of a transparent, beadless fibrous structure. Obtained SEM pictures provide deeper insight into fiber morphology, displaying uniform fibers of smooth surface. Mean fiber diameter was given as 12.1±3.5 µm (n=50). The average drug content was 9.01±0.26% w/w (n=5).

The endothermic peak visible on the thermogram of the physical mixture can be related to the melting point of the crystalline carvedilol, which is missing from the thermogram of the microfibers, therefore crystalline-amorphous transition of the active ingredient could be concluded.

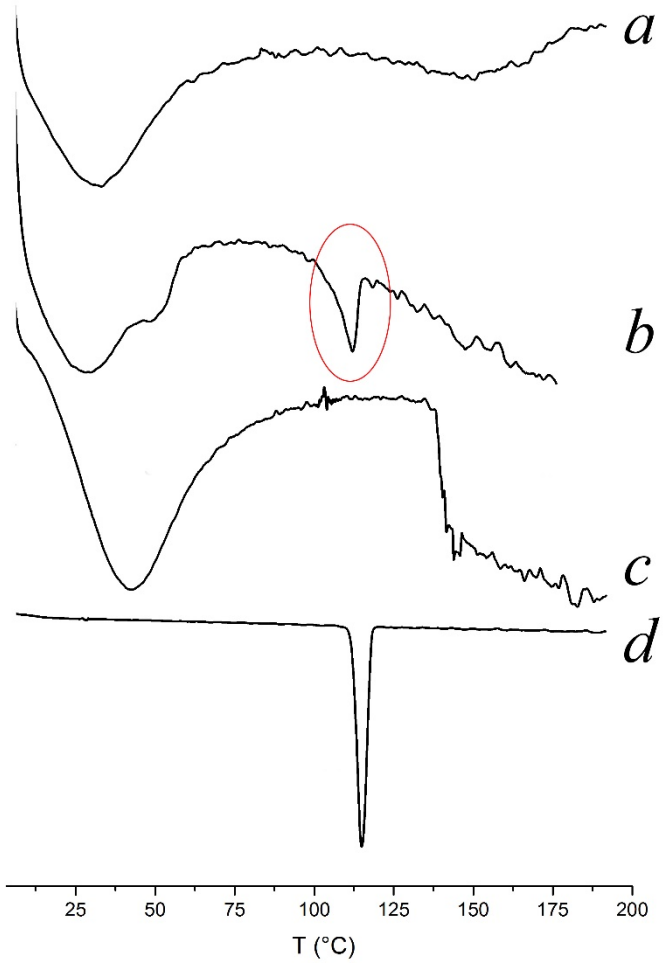

Figure 20 DSC thermograms of investigated samples: *a*: CD loaded microfibers, *b*: physical mixture, *c*: Klucel® ELF type HPC, *d*: crystalline CD

DOI:10.14753/SE.2016.1927

The recorded XRD patterns also confirms the crystalline amorphous transition of CD (Fig. 21). Characteristic high intensity peaks originating from the crystalline CD is clearly detectable on the curves of physical mixture, while with respect to the diffractogram of fibers, only diffuse peaks can be identified.

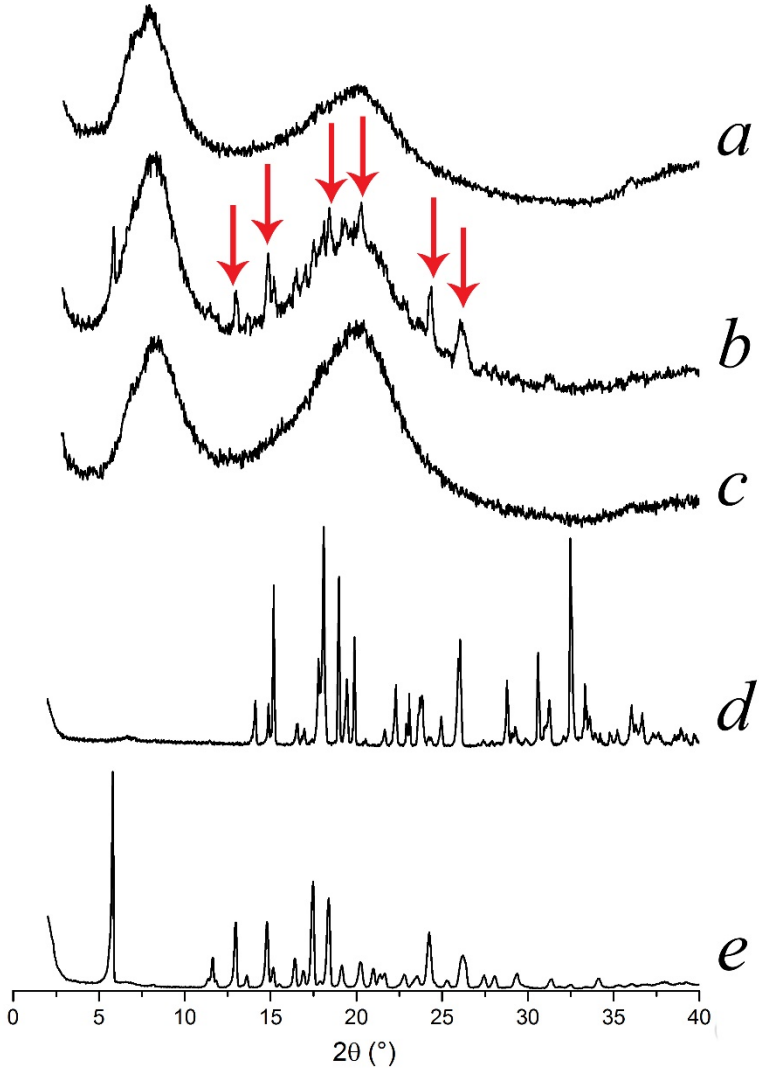

Figure 21 XRD patterns of investigated samples: *a*: CD loaded microfibers, *b*: physical mixture, *c*: Klucel® ELF type HPC, *d*: citric acid monohydrate, *e*: crystalline CD

In accordance with the findings of XRD and DSC, ATR-FTIR measurements also pointed out the crystalline-amorphous transition of CD. The spectrum recorded from physical mixture bears the characteristic features of crystalline CD (-NH stretching vibration at 3200–3300 cm^{-1} and -CH stretching vibrations at 2900–3100 cm^{-1}), whils these peaks cannot be found in the spectrum of microfibers (Fig. 22). The observed phenomenon is

due to the lack of long term ordering specific to crystalline substances, thus enabling much more allowed conformations. The absorbed energy is distributed throughout the many conformations resulting in the merging and broadening of characteristic peaks.

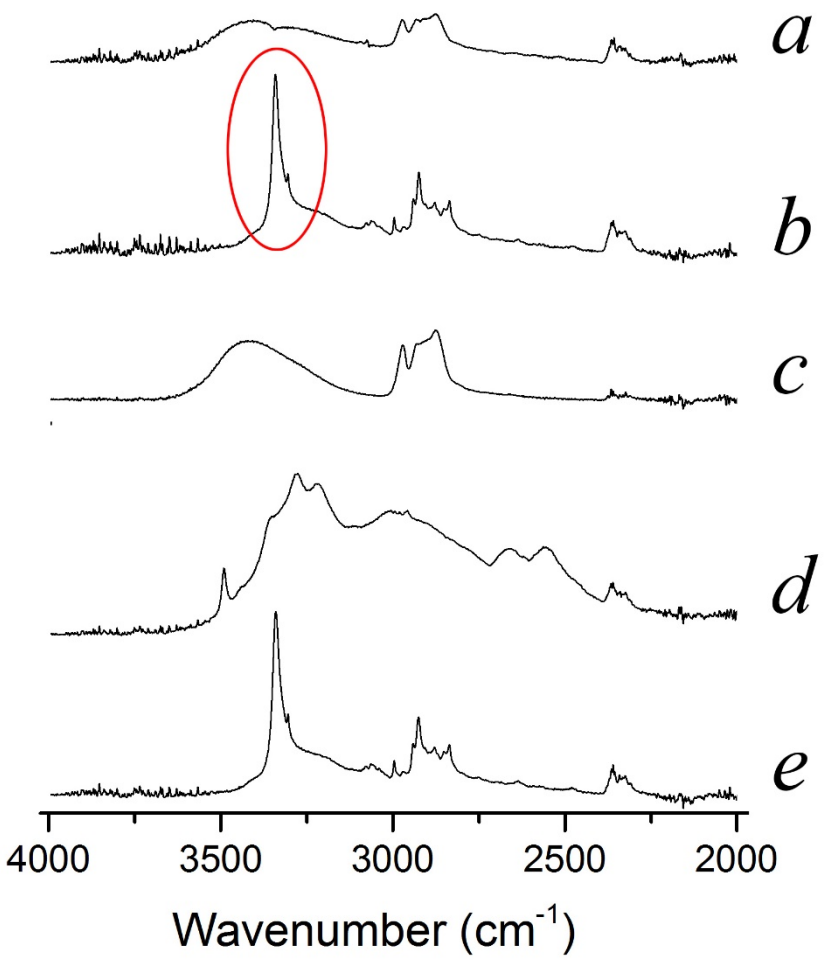

Figure 22 ATR-FTIR spectra of investigated samples: *a*: CD loaded microfibers, *b*: physical mixture, *c*: Klucel® ELF type HPC, *d*: citric acid monohydrate, *e*: crystalline CD

Measurement of o-Ps lifetimes was also carried out, and the results imply a significant change in the supramolecular structure along with the fiber formation. The large reduction in o-Ps lifetime values, thus in the size of free volume holes can be related to the supramolecular ordering of HPC chains (Fig. 23). The reason for this can be found in the crystalline-amorphous transition of CD, and also in the formation of a SS.

DOI:10.14753/SE.2016.1927

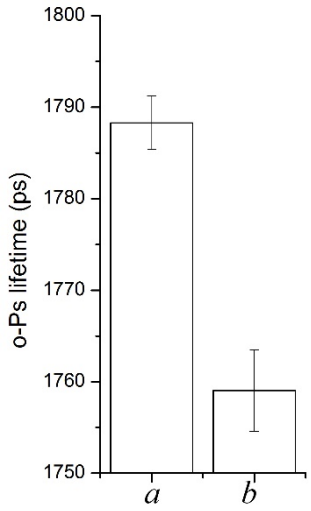

Figure 23 o-Ps lifetime values of physical mixture (a) and CD loaded microfibers (b)

6.3. Formulation and examination of orodispersible tablets

The drug loaded microfibers were intended to be processed into orodispersible tablets. Therefore milling of fibers was necessary in order to obtain pharmaceutically more manageable samples. Along with the microfibers, citric acid monohydrate and sodium bicarbonate was also milled for the enhancement their disintegrating activity.

6.3.1. MD containing orodispersible tablets

The efficacy of the milling process was monitored by particle size measurements, of which results are shown in Table 8. Poly(ethylene glycol) was used as water soluble lubricant, because of its large particle size it was also subjected to milling.

Table 8 Particle size characteristics of milled substances

	Mean size (µm) ± S.D.	**Size distribution span ± S.D.**
MD loaded microfibers	208±10	2.67±0.19
Citric acid, anhydrous	174±58	3.23±0.72
Poly(ethylene glycol) 1500	146±12	1.44±0.14
Sodium bicarbonate	132±1	1.78±0.01

DOI:10.14753/SE.2016.1927

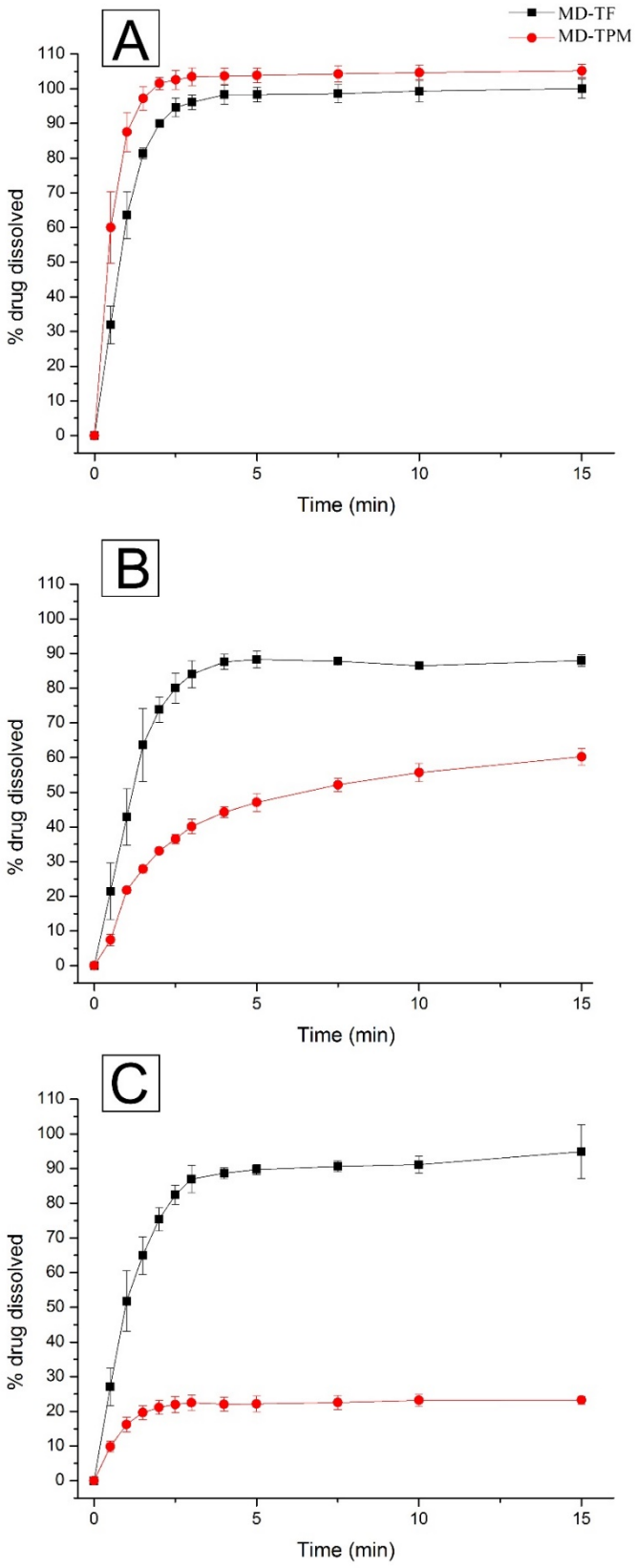

Figure 24 Dissolution profiles of MD containing orodispersible tablets: *A:* pH 1.0, *B:* pH 4.5, *C:* pH 6.8 (n=3)

DOI:10.14753/SE.2016.1927

Table 8 indicates that the size of milled substances are comparable to that of the size of common tableting excipients.

All of the investigated tablet parameters complied with pharmacopoeial and our predetermined requirements, indicating that the tablets possess appropriate mechanical and disintegration properties (Table 9).

Table 9 Tablet characteristics of MD containing orodispersible tablets

Tablet parameter	**MD-TF**		**MD-TPM**	
Hardness (N) ± S.D.	32.2±1.3		32.0±1.9	
Friability (%)	0.39		0.37	
Disintegration time (s)	25.18 (first)	26.72 (last)	25.25 (first)	29.31 (last)
Mass (g) ± S.D.	0.5008±0.0061		0.5029±0.0022	

The performed dissolution tests revealed a considerable difference between the examined formulations (Fig.24). MD release was rapid, complete and almost independent from the pH of the applied medium. In contrast, the pH of the medium had a great impact on the dissolution from the control MD-TPM tablets, resulting their incomplete drug release.

Significant difference was confirmed by the calculated difference and similarity factors shown in Table 10.

Table 10 Calculated difference (f_1) and similarity (f_2) factors

		Test					
		MD-TF					
		f_1			**f_2**		
		pH 1.0	**pH 4.5**	**pH 6.8**	**pH 1.0**	**pH 4.5**	**pH 6.8**
Reference	**MD-TPM**						
	pH 1.0	11.36	15.56	11.38	45.17	44.66	50.77
	pH 4.5	123.33	88.59	97.90	17.42	24.22	22.42
	pH 6.8	323.98	258.02	275.71	10.15	14.62	13.42

6.3.2. CD containing orodispersible tablets

Particle size characteristics of milled substances applied for tableting are shown in Table 11. Based on these results we can conclude that the size of the milled materials is comparable to that of the common tableting excipients. In order to clarify whether fibrous structure could be retained after milling, SEM pictures were recorded too.

Table 11 Particle size characteristics of milled substances

	Mean size (µm) ± S.D.	**Size distribution span ± S.D.**
CD loaded microfibers	135±1	2.85±0.03
Citric acid anhydrous	168±37	2.34±0.31
Sodium bicarbonate	141±19	1.54±0.24

Fig. 25 demonstrates that milling did not deteriorate the basic fibrous structure of our sample, moreover surface crystallization of the active was not observable either. The latter suggests that the chosen milling technique was suitable for the desired purpose.
Both mechanical and disintegration properties were complied with the pharmacopoeial requirements, and there is no remarkable difference between CD-TF and CD-TPM in respect of the investigated parameters (Table 12).

Table 12 Tablet characteristics of CD containing orodispersible tablets

Tablet parameter	**CD-TF**		**CD-TPM**	
Hardness (N) ± S.D.	42.2±2.4		40.3±1.7	
Friability (%)	0.54		0.48	
Disintegration time (s)	27.11 (first)	29.08 (last)	24.47 (first)	28.21 (last)
Mass (g) ± S.D.	0.5997±0.0124		0.6029±0.0102	

Dissolution test of CD containing tablets was carried out in two dissolution media, which unveiled a notable dissimilarity between release profiles. CD release from the fiber based tablets was very fast and complete in each dissolution media, whilst the release profile of

DOI:10.14753/SE.2016.1927

CD-TPM was firmly influenced by the employed dissolution media, resulting a deficient drug release at higher pH values (Fig. 26).

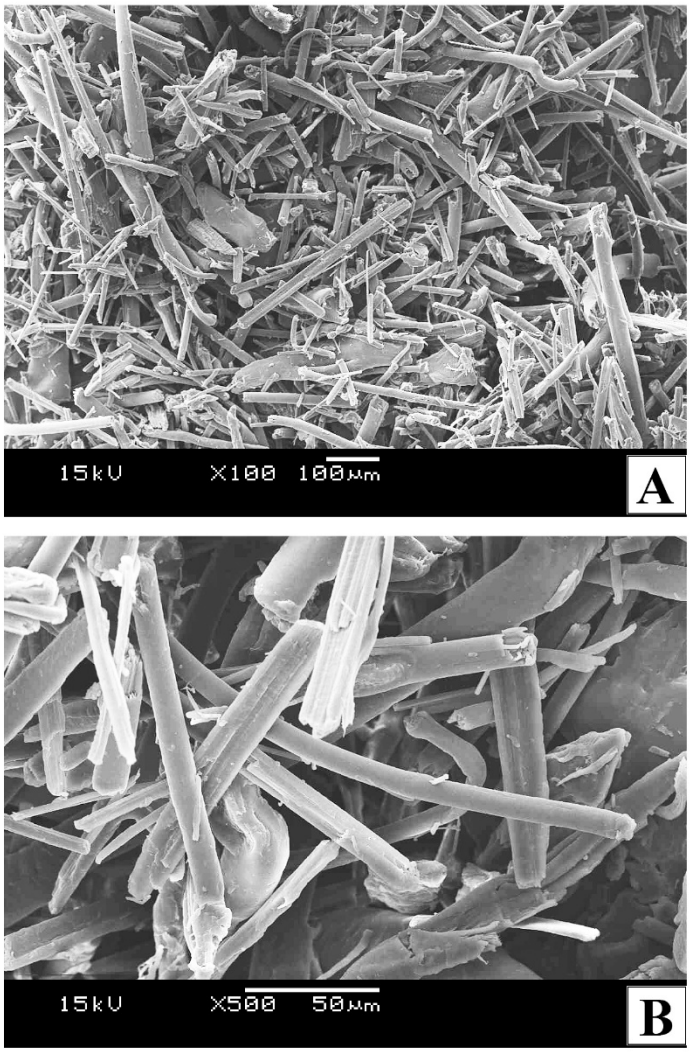

Figure 25 SEM records of milled CD loaded microfibers, A: 100x, B: 500x magnification

Table 13 Calculated difference (f_1) and similarity (f_2) factors

			Test			
			CD-TF			
			pH 1.0		pH 6.8	
			f_1	f_2	f_1	f_2
Reference	CD-TPM	pH 1.0	21.78	39.05	7.89	58.66
		pH 6.8	149.63	13.12	111.62	19.04

DOI:10.14753/SE.2016.1927

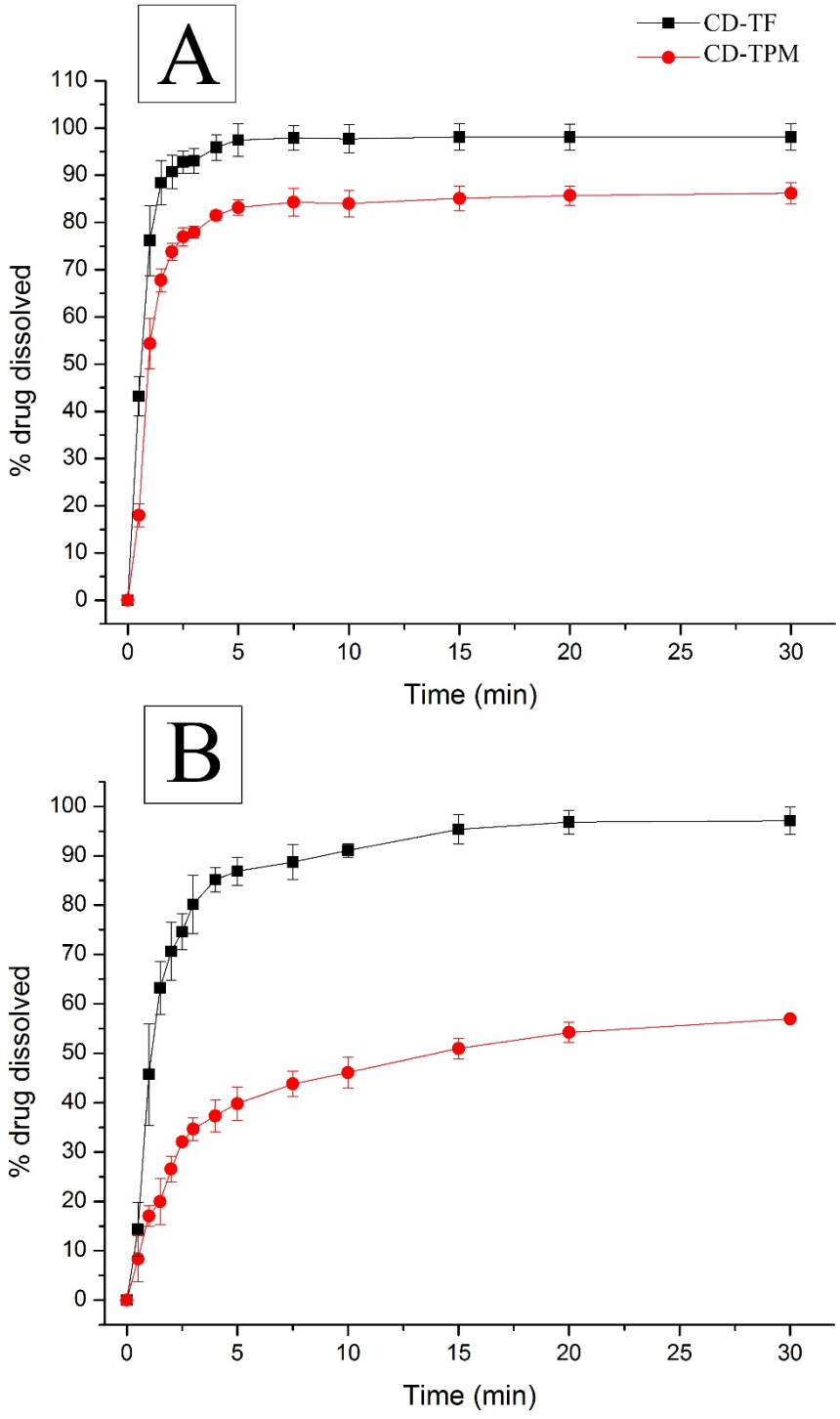

Figure 26 Dissolution profiles of CD containing orodispersible tablets: *A:* pH 1.0, *B:* pH 6.8

The observed difference was either corroborated by the calculated difference and similarity factors listed in Table 13.

6.4. Accelerated stability test

Stability test under stress conditions was conducted in order to gain information on the physicochemical resistance of CD loaded microfibers.

DSC analysis of the stored samples did not revealed any noteworthy change neither from the point of view of crystallinity, nor from the point of view of other solid state property, *e.g.* softening temperature (ca. 140–150 °C) (Fig. 27).

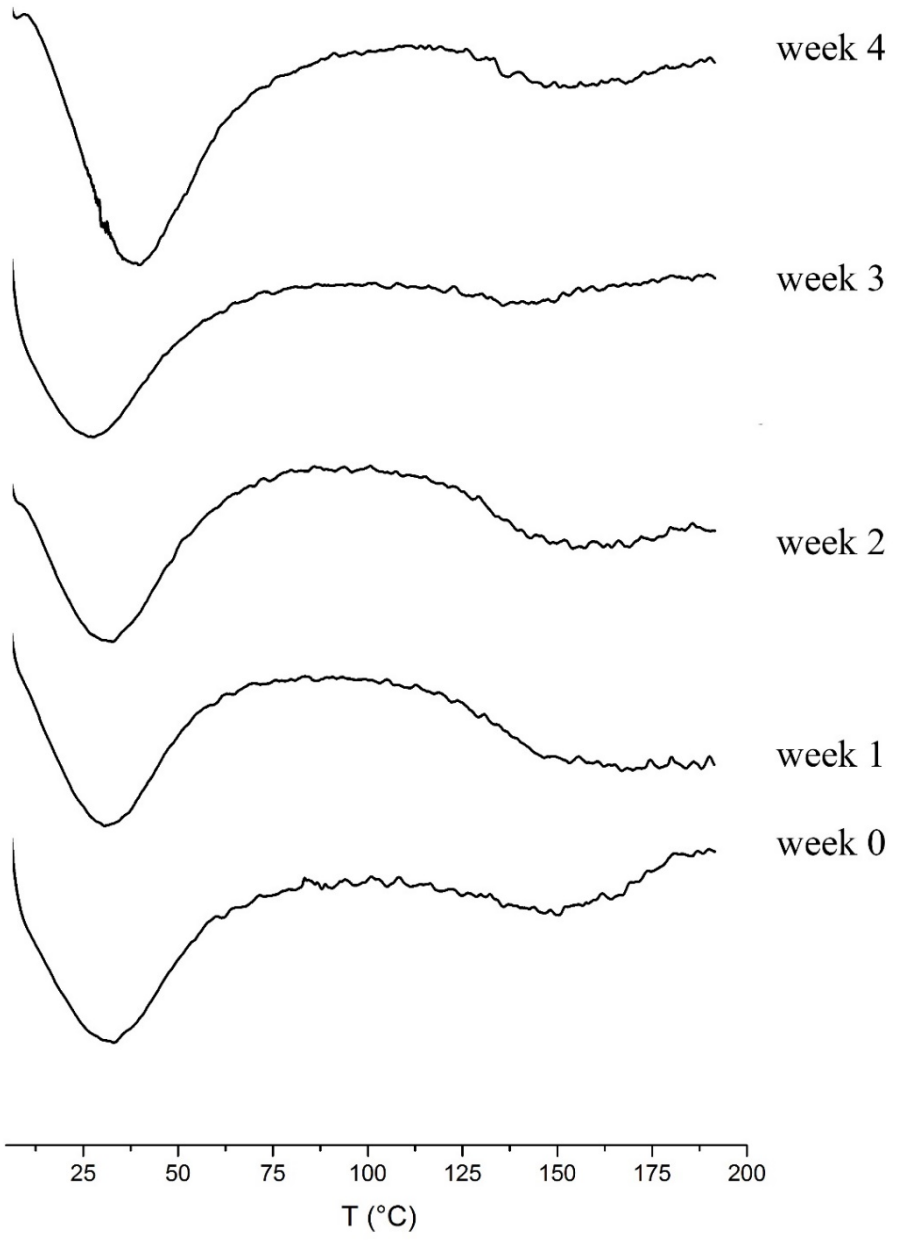

Figure 27 DSC thermogarms of the stored CD loaded microfibers

DOI:10.14753/SE.2016.1927

XRD patterns present a more nuanced insight into physicochemical changes along with the storage time. Considering samples up to week 3, the drug was kept in an unchanged amorphous form embedded in the polymer matrix. But the diffractogram of the fiber stored for 4 weeks have developed slight intensity peaks resembling to that of the CD (Fig. 28). This suggest the partial crystallization amorphous drug.

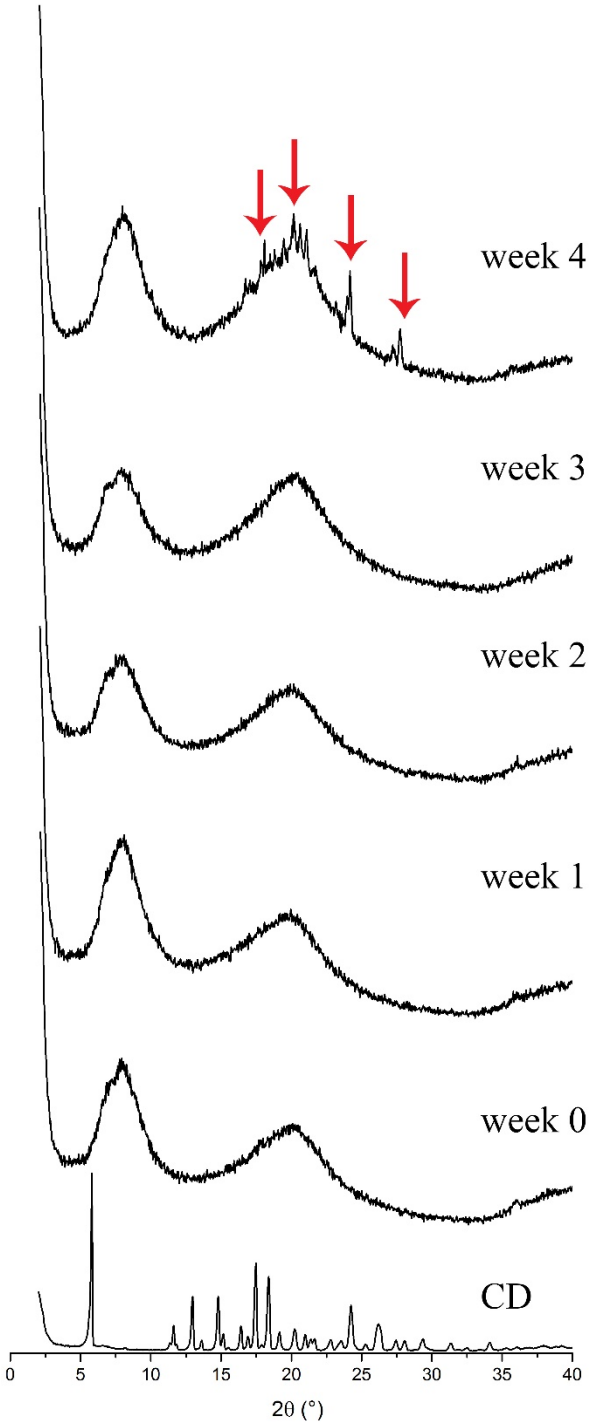

Figure 28 XRD patterns of the stored CD loaded fibers and the crystalline drug substance

In accordance with the findings of XRD patterns, the recorded ATR-FTIR spectra also indicated the partial crystallization of the active. There is no significant difference between the spectra up to week 3. The formation of the characteristic peak at 3200–3300 cm^{-1} (-NH stretching vibration) imply the recrystallization of the incorporated CD in case of sample stored for four weeks (Fig. 29).

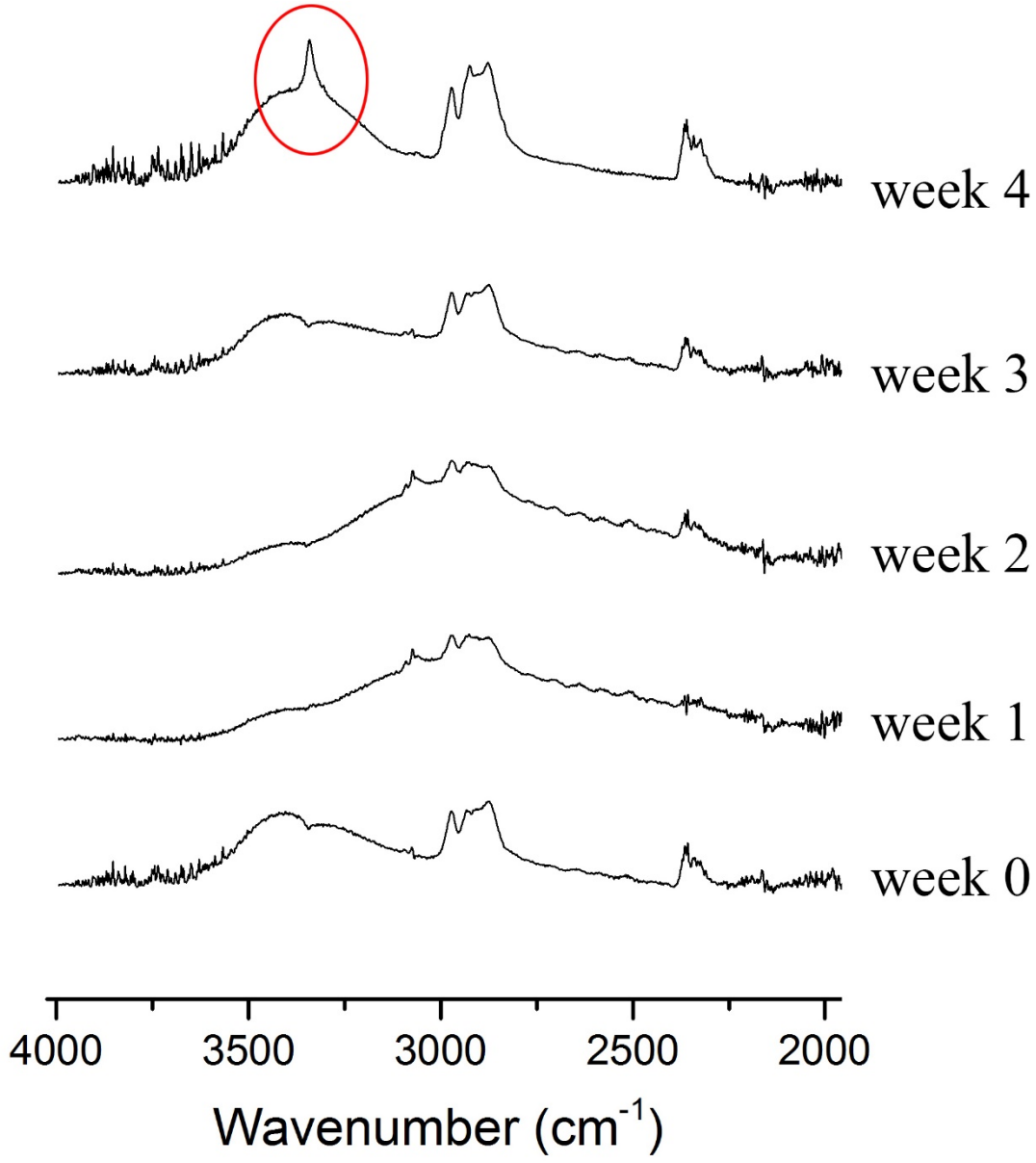

Figure 29 ATR-FTIR spectra of the stored CD loaded microfibers

PALS measurements were also carried out in order to monitor ageing related supramolecular changes. The determined o-Ps lifetime was on the rise along with the

DOI:10.14753/SE.2016.1927

storage time (Fig. 30). This can be traced back to the disturbance of the ordered supramolecular structure, which can be closely related to the recrystallization of CD or the water absorption of polymer chains.

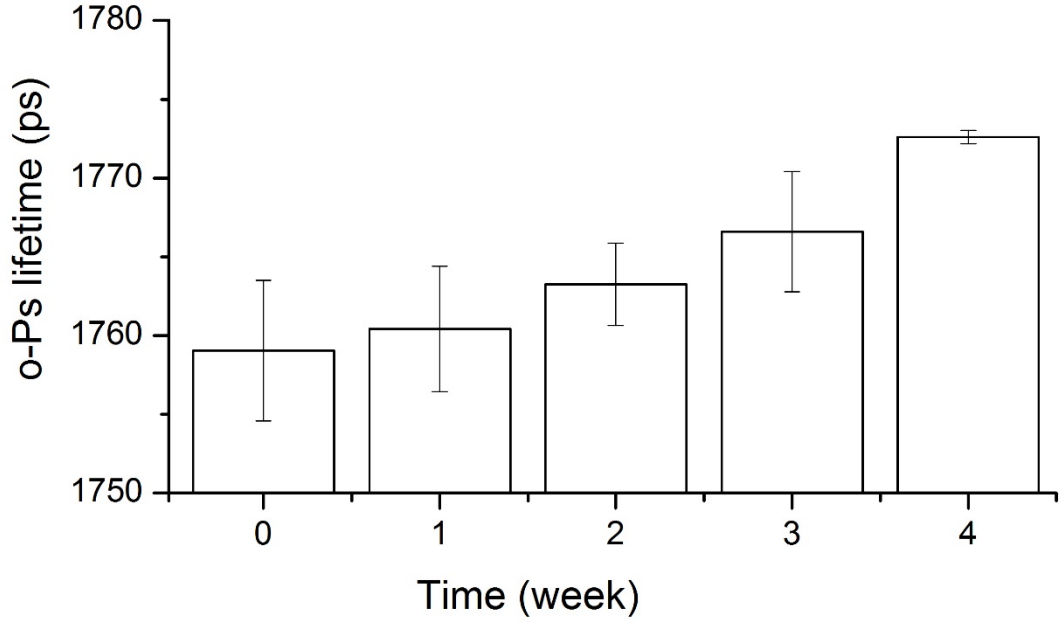

Figure 30 o-Ps lifetime of the freshly prepared and stored CD-loaded microfibers

DOI:10.14753/SE.2016.1927

7. DISCUSSION

7.1. Preformulation study

Suitability of HPC of different molecular weights for high speed rotary spinning was experimentally demonstrated. Applying concentrated aqueous HPC gels, fibers in the range of a few to few tens of micrometers were formed. However, recent research activities in the field of fiber formation focuses mainly on the preparation of nanosized fibers, our further goal was the preparation of fiber based oral drug delivery system containing milled fibers. The processing of nanosized particles is often much more cumbersome (e.g. homogenization with tableting excipients), than particles of a size of microns. The combination of microscopic analysis, monitoring of yield and texture analysis enabled the determination of critical minimum and maximum fiber forming concentrations, as well as the optimum concentration. From the point of yield it is evident that the higher the yield, the better the spinnability of the gel. But with respect to the fiber diameter and adhesiveness the observations need detailed explanations. As described before, high speed rotary spinning calls for viscoelastic gels, where the formed centrifugal force induces the lengthening of the gel jet leaving the wall orifice. Thus a better viscoelastic behavior results in a pronounced elongation and a consequence lower fiber diameter. The narrow distribution of diameters is also a desired property of the prepared fibers. Based on the results of image analysis, the narrowest distribution of fiber diameters were associated with the least mean fiber diameter.

The designed experimental set-up for the textural characterization was intended to mimic this viscoelastic behavior during the fiber formation. Adhesiveness is calculated from that section of the load-distance curve, which is associated to the backward moving of the probe inserted in polymer gel. Thus the “stretching” of the viscoelastic sample could be correlated to the elongation in the course of the fiber formation. Based on these considerations it can be concluded that the lower the adhesiveness, the better the spinnability, since there exists a smaller inner resistance to the induced elongation. Another possible approach to understand the role of adhesiveness in fiber formation comes from the definition of the measured parameter. Adhesiveness represents the work necessary to overcome the attractive forces between two surfaces, it can be easily adapted to the applied spinning system. Therefore, adhesiveness is the work required for the

detachment of gels from the surface of the spinneret, in order to leave the orifices and form jets. Bearing all these considerations and obtained results in mind, it can be seen, that the lower adhesiveness values are more beneficial for high speed rotary spinning.

The results also confirms that spinning properties are affected by not only the concentration, but by the average molecular weight of the polymer. A remarkable difference was also found between the adhesiveness values of Klucel® ELF and EXF, implying that the lager the molecular weight, the higher the adhesiveness.

It has been reported previously, that HPC gels develop liquid crystalline structure which is affected by the polymer content of the gels (Ernst and Navard, 1989). The proposed structure for the aqueous gels was found to be cholesteric (Werbowyj and Gray, 1984). Taking all these into account it can be suggested that the specific shape of the adhesiveness curves is related to the concentration dependent supramolecular structure of HPC gels, which determines its textural properties. In other words, texture analysis enabled the selection of that concentration, at which a supramolecular structure beneficial for fiber formation is formed within the gel.

This liquid crystalline hypothesis is in accordance with former observations published in literature. Canejo *et al.* have demonstrated that electrospinning of liquid crystalline solutions of cellulose derivative results in the formation of helically twisted fibers, which was also observable in our samples (Canejo *et al.*, 2008).

7.2. Preparation and investigation of drug loaded microfibers

The results demonstrated that Klucel® ELF type HPC was a suitable polymer for the incorporation of active ingredients. The obtained average fiber diameters are slightly greater than that of presented in Table 7. The differences can be explained by the changed solvent and by the large amount of drug dissolved in the stock solution used for gel preparation. The introduction of a more volatile solvent (ethanol) into the spinning process, itself causes the thickening of fiber diameter. Rapid evaporation results in the premature solidification of ejected polymer jets leaving no room for the elongation. The use of a concentrated drug stock solution acts in the same way; the less solvent evaporates sooner. Our primary stipulation about formulation of poorly soluble drugs using the fibers based approach was that any kind of potential harm solvents should be avoided. Therefore ethanol, which has been classified as a solvent with low toxic potential (solvent class 3)

was applied (ICH, 2015). Both of the active ingredients are practically insoluble in water, and only slightly soluble in ethanol, hence ethanol alone would not be sufficient for dissolving them. This apparent contradiction was resolved by the exploitation of the weak basic centres of the drugs and the leveling effect of ethanol. Citric acid was capable to dissolve the actives in the presence of ethanol. Our strategy proved effective to circumvent low aqueous solubility without the use of harm solvents.

The recorded microscopic images indicated the formation of a transparent system with lack of any signs of surface crystallization of drugs. The latter suggests that the chosen solvent mixture was appropriate for the spinning process- If the solvent is not a good solvent for one of the components, surface crystallization can take place during the evaporation-solidification (Zeng *et al.*, 2005b).

The performed physicochemical characterization unquestionably pointed out the crystalline-amorphous transition of the incorporated drug. However it is an interesting question that ASD or SS was formed. Based on the available data, we can propose that a SS was formed. The reason for this is could be the transparent nature of the system, and the great extent of o-Ps lifetime reduction (Albers *et al.*, 2009). In SSs, amorphous drug is molecularly dispersed in the polymer matrix, which means that drug molecules wedged between the polymer chains could reduce the size of free volumes (Figure 31).

7.3. Formulation and examination of orodispersible tablets

The experiments were intended to highlight the importance and applicability of fibrous drug delivery systems in oral administration. Microfiber based tablets of appropriate mechanical and disintegration properties were successfully prepared by direct compression, a common tableting procedure. The reason for the simultaneous use of effervescent agent and superdisintegrant was the aim to overcome the large binding force exerted by HPC.

Orodispersible tablets represent a popular dosage form, because of its several benefits, including the ease of administration, rapid disintegration enabling the drug absorption from the proximal sections of the gastrointestinal tract. The latter combined with the dissolution enhancing effect of fibers can result in an improved bioavailability of the drug. The dissolution from the fiber based formulas was rapid, complete and independent from the applied media in respect of each drug. This can be explained by the rapid in vitro

disintegration of the prepared tablets, the high specific surface area of milled fibers and the amorphous state of the incorporated drug. However, microenvironmental modulator effect of the incorporated citric acid in the drug-polymer complex could be also mentioned, since the dissolution of citric acid and drug form microfibers is simultaneous, and spatially related. In case of the control tablets, the drug dissolution was determined by the pH dependent solubility features of the drugs. Since the control and fiber based tablets were very similar in means of tablet parameters, and had the same compositions, the observed differences can be exclusively associated to the microfibers.

The results indicate that this approach can be a useful mean to improve in vitro performance of BCS class II drugs. Since the bioavailability of these drugs is mainly limited by their solubility, the rapid dissolution can result in an improved absorption.

7.4. Accelerated stability test

Stability is an ever critical aspect of formulation of dosage forms. Innovative, novel dosage forms, such as fiber based formulations are particularly watched with eager eyes. Amorphous state is thermodynamically not stable, therefore the stabilization of dosage forms containing amorphous drugs is a challenge.

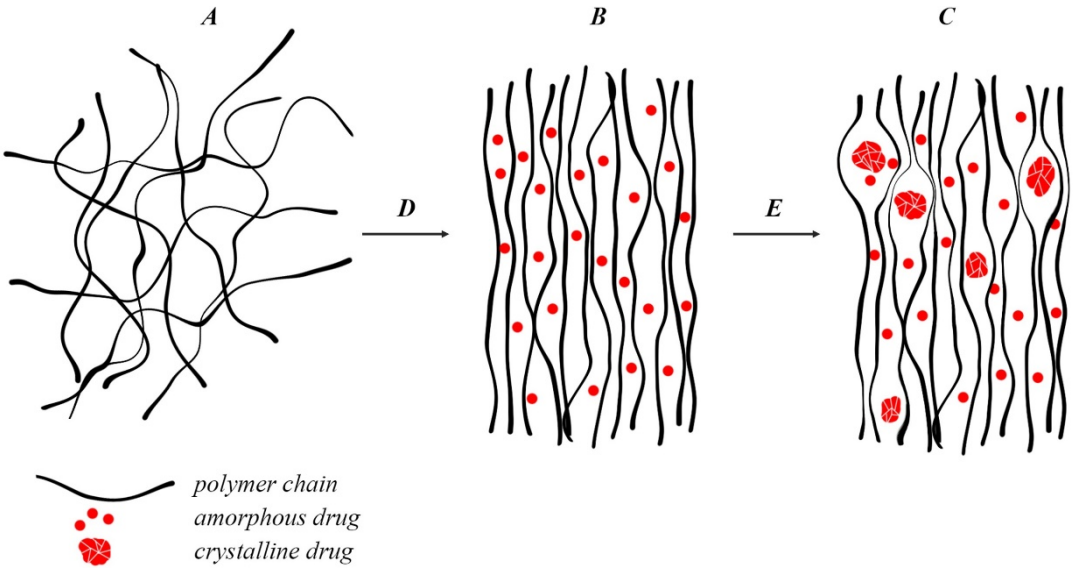

Figure 31 Proposed explanation for the supramolecular changes observed during the stability testing: *A*: raw polymer, *B*: freshly prepared drug loaded microfiber, *C*: stored drug loaded microfiber, *D*: fiber formation, E: storing

DOI:10.14753/SE.2016.1927

The performed physicochemical examinations indicated that along with the time of storage, the drug tended to recrystallize. In respect of ASDs and SSs, molecular mobility plays a pivotal role in the stability, since a reduced molecular mobility does not allow amorphous molecules to aggregate and to form crystals. It has been found that molecular mobility can be decreased by an elevating glass transition temperature of the amorphous system (e.g. with the use of a polymer of a high glass transition temperature). Another key element of the stability of these systems is the formation of strong polymer-drug interactions, which keep the incorporated drug in an amorphous state (Qian *et al.*, 2010). Regarding the results of the accelerated stability test, the temperature dependence of molecular mobility should be considered, as well (Hancock *et al.*, 1995). The observed supramolecular changings along with the storage time can be interpreted as the expanding effect of the recrystallized drug on the polymeric chains (Figure 31).

DOI:10.14753/SE.2016.1927

8. CONCLUSIONS

Because of their advantages in biological and in drug delivery applications, an ever increasing interest has been paid to polymeric fibers. Fiber based formulations have been proved to be a potential approach to address the burning issue of modern pharmacy; *i.e.* poor aqueous solubility. In contrast to electrospinning, high speed rotary spinning represents a less charted area of fiber formation. Thus the impact of solution parameters on fiber formation, the processability of fibers, their applicability in the development of oral dosage forms, and their stability has been not fully understood in details yet. My work summarizes the efforts have been paid to elucidate the role of rotary spun fibers in pharmaceutical technology.

Novelties and the practical relevance of my work are as follows:

- Based on the literature review it was the first time that suitability of two different HPCs (Klucel® EXF and ELF) for high speed rotary spinning with the aim of producing polymer microfibers was demonstrated.
- Novel experimental set-up was introduced to the preformulation studies of high speed rotary spinning; the method was capable to mimic the conditions (elongation of the viscoelastic solution) of the spinning process. Thus a relationship was found between adhesiveness and spinnability; the lower the adhesiveness the better the spinnability. The novel application of textural analysis was first demonstrated for the characterization of spinnability.
- Unique shape of adhesiveness curves of the investigated HPCs was related to the concentration dependent liquid crystalline structure of the aqueous gels. This findings is in strong agreement with previous literature reports.
- The tracking of fiber formation; the determination of critical minimum, maximum and the optimum fiber forming concentrations could be easily established using the combination of microscopic evaluation, monitoring of process yield and textural characterization.
- It was the first reported that drug loaded microfibers were prepared via high speed rotary spinning using actives of BCS class II applying a novel approach. The high speed rotary spinning of polymer gels containing drugs dissolved resulted in the

formation of an amorphous drug delivery system and in the supramolecular ordering of polymer chains.

- The fiber formation was successfully carried out without the employment of any harm solvent. Weak basic feature of drugs could be circumvented by the application of hydroalcoholic solvent mixture and citric acid.
- It was first described that fibrous structure of drug loaded microfibers can be retained after milling by rotary knife grinder.
- Novel orodispersible tablets, containing milled microfibers possessing satisfying features in terms of mechanical properties and in vitro disintegration were prepared. The combination of milled drug loaded microfibers with common tableting excipients enabled the preparation of orodispersible tablets by direct compression.
- The novelty of the work was the pH independent (in the pH range of 1.0-6.8), rapid and complete drug dissolution from microfiber based orodispersible tablets. Explanation of these observations were the high specific surface of microfibers, amorphous state of active ingredient, the acidic microenvironmental modulator effect of citric acid in the polymer-drug complex and the rapid disintegration of the compressed tablets.
- It was the first time, to the best to our knowledge, that physicochemical stability related data on rotary spun drug loaded microfibers was reported. Physicochemical stability of drug loaded microfibers is still a challenge and is influenced by several factors. Carvedilol loaded microfibers exhibited good stress tolerance capacity. Despite all of these, partial recrystallization took place by the end of the storage.

DOI:10.14753/SE.2016.1927

9. SUMMARY

In this work, a rotary spun microfiber based formulation was demonstrated and discussed in details from the preformulation studies through tablet formulation to the stability testing.

HPC, semisynthetic derivative of cellulose was selected for fiber formation, and this was the first time to demonstrate its spinnability via high speed rotary spinning. Preformulation studies of two HPCs of different average molecular weights were carried out by the monitoring of fiber morphology, of process yield, as well as of adhesiveness. In the course of texture analysis a relationship was found between spinnability and adhesiveness: the lower the adhesiveness, the better the spinnability. Reason for the specific shape of the adhesiveness curves was identified as the formation of liquid crystalline structure in concentrated gels of HPC.

Drug loaded fibers were successfully manufactured employing Klucel® ELF and actives selected from BCS class II. Dissolution of drugs in an organic solvent, which is the reigning approach for preparing fibers loaded with poorly soluble drugs, was successfully circumvented by the application of hydroalcoholic mixture as solvent and citric acid as hydrotropic agent.

Amorphous transitions of the incorporated drugs were confirmed and supramolecular changes of the polymeric carrier were also monitored.

Milling of microfibers enabled the formulation of orodispersible tablets by direct compression. Blending milled microfibers with common tableting ingredients was sufficient to prepare tablets with desired mechanical and disintegration properties, which complied with pharmacocopeial requirements.

The performed dissolution studies in different dissolution media of biorelevant pH values revealed a significant difference between fiber based and control formulations. The drug release of the fiber based formulations was rapid, complete and pH independent.

Accelerated stability test indicated good stress tolerance capacity of CD loaded microfibers, however partial recrystallization of the drug was detectable at the last sampling point.

The results widely demonstrate the applicability of polymer microfibers in the formulation of poorly soluble drugs.

DOI:10.14753/SE.2016.1927

9. ÖSSZEFOGLALÁS

Értekezésemben a polimer mikroszál alapú formulációban rejlő gyógyszerészeti lehetőségekre szerettem volna felhívni a figyelmet. Annak érdekében, hogy a folyamatról átfogó képet nyújtsak az elvégzett kísérletek a preformulációs vizsgálatoktól az orodiszperz tabletták formulálásán át a stabilitás vizsgálatig terjednek.

Munkám során egy, a nagy sebességű szálképzésben mindezidáig nem alkalmazott polimert, a hidroxi-propil-cellulózt (HPC), egy félszintetikus cellulóz származékot alkalmaztam. A preformulációs vizsgálatban két különböző átlagos molekulamérettel jellemezhető HPC-t használtam, mely a szálmorfológia, a folyamatkitermelés, és az előállított gélek adhezivitás értékének elemzésén alapult. A gélek állományelemzése során kapcsolatot találtam az adhezivitás és a szálképzési tulajdonság között, méghozzá minél kisebb az adhezivitás, annál kedvezőbb a szálképzési képesség.

A Biofarmáciai Osztályozási Rendszer 2. osztályába tartozó farmakonokkal sikeresen állítottam elő hatóanyag tartalmú szálakat Klucel® ELF polimerből. A konvencionálisan alkalmazott megközelítést, azaz a vízben rosszul oldódó hatóanyag szerves oldószerben történő oldását sikerült megkerülni hidroalkoholos oldószerelegynek, mint nivelláló oldószernek és citromsavnak, mint hidrotróp oldásközvetítő anyagnak az alkalmazásával.

A hatóanyagok kristályos-amorf átalakulását több fizikokémiai vizsgáló módszerrel is igazoltam, valamint a polimer hordozó szupramolekuláris szerkezetében bekövetkező változásokat is nyomon követtem.

A mikroszálak őrlése lehetővé tette a gyógyszerkönyvi előírásoknak megfelelő mechanikai és dezintegrációs tulajdonságokkal rendelkező szájban szétesző tabletták formulációját közvetlen préselés segítségével.

A bioreleváns kémhatású kioldó közegben végzett kioldódás vizsgálatok szignifikáns különbséget jeleztek a szál alapú és a kontroll tabletták kioldódása között. A mikroszál alapú tabletták esetén a kioldódás gyors, teljes és pH független volt, szemben a kontroll tabletták kioldódásával.

A gyorsított stabilitásvizsgálat során a mikroszálaknak jó stressz tűrő kapacitása volt, ugyanakkor az utolsó mintavételi pontnál a hatóanyag részleges kikristályosodására utaló jelek is megfigyelhetőek voltak.

10. REFERENCES

Adeli E. (2015) Irbesartan-loaded electrospun nanofibers-based PVP K90 for the drug dissolution improvement: Fabrication, in vitro performance assessment, and in vivo evaluation. J Appl Polym Sci, 132: 42212 (online).

Ahmed I., Nafadi M., Fatahalla F. (2006) Formulation of a fast-dissolving ketoprofen tablet using freeze-drying in blisters technique. Drug Dev Ind Pharm, 32: 437-442.

Albers J., Alles R., Matthée K., Knop K., Nahrup J. S., Kleinebudde P. (2009) Mechanism of drug release from polymethacrylate-based extrudates and milled strands prepared by hot-melt extrusion. Eur J Pharm Biopharm, 71: 387-394.

Aldén M., Tegenfeldt J., Saers E. S. (1993) Structures formed by interactions in solid dispersions of the system polyethylene glycol-griseofulvin with charged and non charged surfactants added. Int J Pharm, 94: 31-38.

Amidon G. L., Lennernas H., Shah V. P., Crison J. R. (1995) A Theoretical Basis for a Biopharmaceutic Drug Classification: The Correlation of in Vitro Drug Product Dissolution and in Vivo Bioavailability. Pharm Res, 12: 413-420.

Andrews G. P., Abu-Diak O., Kusmanto F., Hornsby P., Hui Z., Jones D. S. (2010) Physicochemical characterization and drug-release properties of celecoxib hot-melt extruded glass solutions. J Pharm Parmacol, 62: 1580-1590.

Badrossamay M. R., McIlwee H. A., Goss J. A., Parker K. K. (2010) Nanofiber Assembly by Rotary Jet-Spinning. Nano Lett, 10: 2257-2261.

Bansal K., Pant P., Rao P., Padhee K., Sathapathy A., Kochhar P. S. (2011) Micronization and dissolution enhancement of Norethindrone. Int J Res Pharm Chem, 1: 315-319.

Benet L. Z., Wu C.-Y., Hebert M. F., Wacher V. J. (1996) Intestinal drug metabolism and antitransport processes: A potential paradigm shift in oral drug delivery. J Control Release, 39: 139-143.

Bhardwaj N., Kundu S. C. (2010) Electrospinning: A fascinating fiber fabrication technique. Biotechnol Adv, 28: 325-347.

Bhattarai N., Edmondson D., Veiseh O., Matsen F. A., Zhang M. (2005) Electrospun chitosan-based nanofibers and their cellular compatibility. Biomaterials, 26: 6176-6184.

Boland E. D., Wnek G. E., Simpson D. G., Pawlowski K. J., Bowlin G. L. (2001) Tailoring tissue engineering scaffolds using electrostatic Processing techniques: A study of poly(glycolic acid) Electrospinning. J Macromol Sci A, 38: 1231-1243.

Bonino C. A., Krebs M. D., Saquing C. D., Jeong S. I., Shearer K. L., Alsberg E., Khan S. A. (2011) Electrospinning alginate-based nanofibers: From blends to crosslinked low molecular weight alginate-only systems. Carbohydr Polym, 85: 111-119.

Bravo-Osuna I., Vauthier C., Chacun H., Ponchel G. (2008) Specific permeability modulation of intestinal paracellular pathway by chitosan-poly(isobutylcyanoacrylate) core-shell nanoparticles. Eur J Pharm Biopharm, 69: 436-444.

Breitenbach J. (2002) Melt extrusion: from process to drug delivery technology. Eur J Pharm Biopharm, 54: 107-117.

Broadhead J., Edmond Rouan S. K., Rhodes C. T. (1992) The spray drying of pharmaceuticals. Drug Dev Ind Pharm, 18: 1169-1206.

Brough C., Williams Iii R. O. (2013) Amorphous solid dispersions and nano-crystal technologies for poorly water-soluble drug delivery. Int J Pharm, 453: 157-166.

Brouwers J., Brewster M. E., Augustijns P. (2009) Supersaturating drug delivery systems: The answer to solubility-limited oral bioavailability? J Pharm Sci, 98: 2549-2572.

Brunner E. (1904) Reaktionsgeschwindigkeit in heterogenen Systemen. Z Phys Chem, 43: 56-102.

Canejo J. P., Borges J. P., Godinho M. H., Brogueira P., Teixeira P. I. C., Terentjev E. M. (2008) Helical Twisting of Electrospun Liquid Crystalline Cellulose Micro- and Nanofibers. Adv Mater, 20: 4821-4825.

Chen H., Khemtong C., Yang X., Chang X., Gao J. (2011) Nanonization strategies for poorly water-soluble drugs. Drug Discov Today, 16: 354-360.

Chiou W. L., Riegelman S. (1971) Pharmaceutical applications of solid dispersion systems. J Pharm Sci, 60: 1281-1302.

Crowley M. M., Zhang F., Repka M. A., Thumma S., Upadhye S. B., Kumar Battu S., McGinity J. W., Martin C. (2007) Pharmaceutical Applications of Hot-Melt Extrusion: Part I. Drug Dev Ind Pharm, 33: 909-926.

Cui W., Li X., Zhu X., Yu G., Zhou S., Weng J. (2006) Investigation of Drug Release and Matrix Degradation of Electrospun Poly(dl-lactide) Fibers with Paracetanol Inoculation. Biomacromolecules, 7: 1623-1629.

Deng Q., Jean Y. C. (1993) Free-volume distributions of an epoxy polymer probed by positron annihilation: pressure dependence. Macromolecules, 26: 30-34.

Djuric, D., Fischer, F., Seidel, K., Kolter, K. (2010) The 37th Annual Meeting and Exposition of the Controlled Release Society: Analytical differentiation between solid solutions and solid dispersions of polyvinyl caprolactam - polyvinyl acetate - polyethylene glycol graft copolymer and itraconazole. ; http://www.pharma-ingredients.basf.com/documents/enp/poster/en/gempmd300.pdf; accessed at: 22. 02. 2016.

Dokoumetzidis A., Macheras P. (2006) A century of dissolution research: From Noyes and Whitney to the Biopharmaceutics Classification System. Int J Pharm, 321: 1-11.

Dong B., Arnoult O., Smith M. E., Wnek G. E. (2009) Electrospinning of Collagen Nanofiber Scaffolds from Benign Solvents. Macromol Rapid Commun, 30: 539-542.

Dong Y. X., Liao S., Ramakrishna S., Chan C. K. (2008) Distinctive degradation behaviors of electrospun PGA, PLGA and P (LLA-CL) nanofibers cultured with/without cell culture. Adv Mat Res, 47: 1327-1330.

Edward J. T. (1970) Molecular volumes and the Stokes-Einstein equation. J Chem Educ, 47: 261-270.

El-Badry M., Fathy M. (2006) Enhancement of the dissolution and permeation rates of meloxicam by formation of its freeze-dried solid dispersions in polyvinylpyrrolidone K-30. Drug Dev Ind Pharm, 32: 141-150.

Ernst B., Navard P. (1989) Band textures in mesomorphic (hydroxypropyl) cellulose solutions. Macromolecules, 22: 1419-1422.

Fang J., Niu H., Lin T., Wang X. (2008) Applications of electrospun nanofibers. Chin Sci Bull, 53: 2265-2286.

Fang X., Reneker D. H. (1997) DNA fibers by electrospinning. J Macromol Sci B, 36: 169-173.

FDA/U.S. Food and Drug Administration. (2016) New Molecular Entity (NME) Drug and New Biologic Approvals; http://www.fda.gov/Drugs/DevelopmentApprovalProcess/HowDrugsareDevelopedandApproved/DrugandBiologicApprovalReports/NDAandBLAApprovalReports/ucm373413.htm; accessed at: 22. 02. 2016.

Frenot A., Chronakis I. S. (2003) Polymer nanofibers assembled by electrospinning. Curr Opin Colloid Interface Sci, 8: 64-75.

Frishman W. H. (1998) Carvedilol. N Engl J Med, 339: 1759-1765.

Geng X., Kwon O.-H., Jang J. (2005) Electrospinning of chitosan dissolved in concentrated acetic acid solution. Biomaterials, 26: 5427-5432.

Guzmán H. R., Tawa M., Zhang Z., Ratanabanangkoon P., Shaw P., Gardner C. R., Chen H., Moreau J.-P., Almarsson Ö., Remenar J. F. (2007) Combined use of crystalline salt forms and precipitation inhibitors to improve oral absorption of celecoxib from solid oral formulations. J Pharm Sci, 96: 2686-2702.

Hajiali H., Shahgasempour S., Naimi-Jamal M. R., Peirovi H. (2011) Electrospun PGA/gelatin nanofibrous scaffolds and their potential application in vascular tissue engineering. Int J Nanomedicine, 6: 2133-2141.

Hancock B. C., Shamblin S. L., Zografi G. (1995) Molecular mobility of amorphous pharmaceutical solids below their glass transition temperatures. Pharm Res, 12: 799-806.

Hann M. M. (2011) Molecular obesity, potency and other addictions in drug discovery. Med Chem Comm 2: 349-355.

Hann M. M., Keseru G. M. (2012) Finding the sweet spot: the role of nature and nurture in medicinal chemistry. Nat Rev Drug Discov, 11: 355-365.

Hay E. D. Cell biology of extracellular matrix. Springer Science & Business Media, New York, 2013: 7-40.

Hebert M. F., Roberts J. P., Prueksaritanont T., Benet L. Z. (1992) Bioavailability of cyclosporine with concomitant rifampin administration is markedly less than predicted by hepatic enzyme induction. Clin Pharmacol Ther, 52: 453-457.

Hecq J., Deleers M., Fanara D., Vranckx H., Amighi K. (2005) Preparation and characterization of nanocrystals for solubility and dissolution rate enhancement of nifedipine. Int J Pharm, 299: 167-177.

Hörter D., Dressman J. B. (2001) Influence of physicochemical properties on dissolution of drugs in the gastrointestinal tract1. Adv Drug Deliver Rev, 46: 75-87.

ICH/The International Conference on Harmonisation of Technical Requirements for Registration of Pharmaceuticals for Human Use. (2015) ICH guideline Q3C (R5) on impurities: guideline for residual solvents http://www.ema.europa.eu/docs/en_GB/document_library/Scientific_guideline/2011/03/WC500104258.pdf; accessed at: 22.02.2016.

Ito A., Watanabe T., Yada S., Hamaura T., Nakagami H., Higashi K., Moribe K., Yamamoto K. (2010) Prediction of recrystallization behavior of troglitazone/polyvinylpyrrolidone solid dispersion by solid-state NMR. Int J Pharm, 383: 18-23.

Jacobs T., De Geyter N., Morent R., Desmet T., Dubruel P., Leys C. (2011) Plasma treatment of polycaprolactone at medium pressure. Surf Coat Technol, 205: 543-547.

Jamei M., Turner D., Yang J., Neuhoff S., Polak S., Rostami-Hodjegan A., Tucker G. (2009) Population-Based Mechanistic Prediction of Oral Drug Absorption. AAPS J, 11: 225-237.

Janssens S., Van den Mooter G. (2009) Review: physical chemistry of solid dispersions. J Pharm Parmacol, 61: 1571-1586.

Jeong S. I., Krebs M. D., Bonino C. A., Khan S. A., Alsberg E. (2010) Electrospun Alginate Nanofibers with Controlled Cell Adhesion for Tissue Engineeringa. Macromol Biosci, 10: 934-943.

Ji Y., Ghosh K., Shu X. Z., Li B., Sokolov J. C., Prestwich G. D., Clark R. A. F., Rafailovich M. H. (2006) Electrospun three-dimensional hyaluronic acid nanofibrous scaffolds. Biomaterials, 27: 3782-3792.

Jiang J., Xie J., Ma B., Bartlett D. E., Xu A., Wang C. H. (2014) Mussel-inspired protein-mediated surface functionalization of electrospun nanofibers for pH-responsive drug delivery. Acta Biomater, 10: 1324-1332.

Jiang Y.-N., Mo H.-Y., Yu D.-G. (2012) Electrospun drug-loaded core–sheath PVP/zein nanofibers for biphasic drug release. Int J Pharm, 438: 232-239.

Karavas E., Ktistis G., Xenakis A., Georgarakis E. (2006) Effect of hydrogen bonding interactions on the release mechanism of felodipine from nanodispersions with polyvinylpyrrolidone. Eur J Pharm Biopharm, 63: 103-114.

Kataria K., Sharma A., Garg T., K Goyal A., Rath G. (2014) Novel technology to improve drug loading in polymeric nanofibers. Drug Deliv Lett, 4: 79-86.

Kaukonen A. M., Laitinen L., Salonen J., Tuura J., Heikkilä T., Limnell T., Hirvonen J., Lehto V.-P. (2007) Enhanced in vitro permeation of furosemide loaded into thermally carbonized mesoporous silicon (TCPSi) microparticles. Eur J Pharm Biopharm, 66: 348-356.

Kayser O., Olbrich C., Yardley V., Kiderlen A. F., Croft S. L. (2003) Formulation of amphotericin B as nanosuspension for oral administration. Int J Pharm, 254: 73-75.

Keck C. M., Müller R. H. (2006) Drug nanocrystals of poorly soluble drugs produced by high pressure homogenisation. Eur J Pharm Biopharm, 62: 3-16.

Kenawy E.-R., Abdel-Hay F. I., El-Newehy M. H., Wnek G. E. (2007) Controlled release of ketoprofen from electrospun poly(vinyl alcohol) nanofibers. Mater Sci Eng A, 459: 390-396.

Kim C.-W., Kim D.-S., Kang S.-Y., Marquez M., Joo Y. L. (2006) Structural studies of electrospun cellulose nanofibers. Polymer (Guildf), 47: 5097-5107.

Kim C. W., Frey M. W., Marquez M., Joo Y. L. (2005) Preparation of submicron-scale, electrospun cellulose fibers via direct dissolution. J Polym Sci B Polym Phys, 43: 1673-1683.

Kim H. S., Yoo H. S. (2010) MMPs-responsive release of DNA from electrospun nanofibrous matrix for local gene therapy: In vitro and in vivo evaluation. J Control Release, 145: 264-271.

Kirkegaard P., Eldrup M., Mogensen O. E., Pedersen N. J. (1981) Program system for analysing positron lifetime spectra and angular correlation curves. Comput Phys Commun, 23: 307-335.

Konig C., Ruffieux K., Wintermantel E., Blaser J. (1997) Autosterilization of biodegradable implants by injection molding process. J Biomed Mater Res, 38: 115-119.

Leach A. G., Jones H. D., Cosgrove D. A., Kenny P. W., Ruston L., MacFaul P., Wood J. M., Colclough N., Law B. (2006) Matched Molecular Pairs as a Guide in the Optimization of Pharmaceutical Properties; a Study of Aqueous Solubility, Plasma Protein Binding and Oral Exposure. J Med Chem, 49: 6672-6682.

Li D., McCann J. T., Xia Y. (2005) Use of electrospinning to directly fabricate hollow nanofibers with functionalized inner and outer surfaces. Small, 1: 83-86.

Li J., He A., Han C. C., Fang D., Hsiao B. S., Chu B. (2006) Electrospinning of Hyaluronic Acid (HA) and HA/Gelatin Blends. Macromol Rapid Commun, 27: 114-120.

Li Y., Pang H., Guo Z., Lin L., Dong Y., Li G., Lu M., Wu C. (2014) Interactions between drugs and polymers influencing hot melt extrusion. J Pharm Parmacol, 66: 148-166.

Lipinski C. A. (2000) Drug-like properties and the causes of poor solubility and poor permeability. J Pharmacol Toxicol, 44: 235-249.

Lipinski C. A., Lombardo F., Dominy B. W., Feeney P. J. (2012) Experimental and computational approaches to estimate solubility and permeability in drug discovery and development settings. Adv Drug Deliver Rev, 64, Supplement: 4-17.

Liu S.-J., Kau Y.-C., Chou C.-Y., Chen J.-K., Wu R.-C., Yeh W.-L. (2010) Electrospun PLGA/collagen nanofibrous membrane as early-stage wound dressing. J Memb Sci, 355: 53-59.

Liu S., Wang X., Zhang Z., Zhang Y., Zhou G., Huang Y., Xie Z., Jing X. (2015a) Use of asymmetric multilayer polylactide nanofiber mats in controlled release of drugs and prevention of liver cancer recurrence after surgery in mice. Nanomedicine, 11: 1047-1056.

Liu W., Chen X. D., Selomulya C. (2015b) On the spray drying of uniform functional microparticles. Particuology, 22: 1-12.

Liu Y., Chen J., Misoska V., Wallace G. G. (2007) Preparation of novel ultrafine fibers based on DNA and poly(ethylene oxide) by electrospinning from aqueous solutions. React Funct Polym, 67: 461-467.

Liu Y., Ma G., Fang D., Xu J., Zhang H., Nie J. (2011) Effects of solution properties and electric field on the electrospinning of hyaluronic acid. Carbohydr Polym, 83: 1011-1015.

Maggi L., Canobbio A., Bruni G., Musitelli G., Conte U. (2015) Improvement of the dissolution behavior of gliclazide, a slightly soluble drug, using solid dispersions. J Drug Deliv Sci Tec, 26: 17-23.

Maretschek S., Greiner A., Kissel T. (2008) Electrospun biodegradable nanofiber nonwovens for controlled release of proteins. J Control Release, 127: 180-187.

Mauludin R., Müller R. H., Keck C. M. (2009) Kinetic solubility and dissolution velocity of rutin nanocrystals. Eur J Pharm Sci, 36: 502-510.

Merisko-Liversidge E., Liversidge G. G. (2011) Nanosizing for oral and parenteral drug delivery: A perspective on formulating poorly-water soluble compounds using wet media milling technology. Adv Drug Deliver Rev, 63: 427-440.

Monnier X., Delpouve N., Basson N., Guinault A., Domenek S., Saiter A., Mallon P. E., Dargent E. (2015) Molecular dynamics in electrospun amorphous plasticized polylactide fibers. Polymer (Guildf), 73: 68-78.

Moore J. W., Flanner H. H. (1996) Mathematical Comparison of Dissolution Profiles. Pharm Technol, 20: 64-74.

Morgan T. (1994) Clinical Pharmacokinetics and Pharmacodynamics of Carvedilol. Clin Pharmacokinet, 26: 335-346.

Müller C., Ulrich J. (2012) The dissolution phenomenon of lysozyme crystals. Cryst Res Technol, 47: 169-174.

Müller R. H., Böhm B. H. L., Grau M. J. Nanosuspensions: A formulation approach for poorly soluble and poorly bioavailable drugs. In: Wise, D. L. (ed.), Handbook of pharmaceutical controlled release technology. Marcel Dekker, New York, 2000:345–357.

Nayak R., Padhye R., Kyratzis I. L., Truong Y., Arnold L. (2011) Recent advances in nanofibre fabrication techniques. Text Res J, 129-147.

Nernst W. (1904) Theorie der Reaktionsgeschwindigkeit in heterogenen Systemen. Z Phys Chem, 47: 52-55.

Newman A., Nagapudi K., Wenslow R. (2015) Amorphous solid dispersions: a robust platform to address bioavailability challenges. Ther Deliv, 6: 247-261.

Nie H., He A., Zheng J., Xu S., Li J., Han C. C. (2008) Effects of Chain Conformation and Entanglement on the Electrospinning of Pure Alginate. Biomacromolecules, 9: 1362-1365.

Noyes A. A., Whitney W. R. (1897) The rate of solution of solid substances in their own solutions. J Am Chem Soc, 19: 930-934.

Oetjen G.-W., Haseley P. Pharmaceutical, Biological and Medical Products. In: Oetjen, G.-W.,Haseley, P. (ed.), Freeze-Drying. Wiley-VCH Verlag, Weinheim, 2007:295-344.

Ohkawa K., Cha D., Kim H., Nishida A., Yamamoto H. (2004) Electrospinning of Chitosan. Macromol Rapid Commun, 25: 1600-1605.

Özdemir N., Ordu S., Özkan Y. (2000) Studies of Floating Dosage Forms of Furosemide: In Vitro and In Vivo Evaluations of Bilayer Tablet Formulations. Drug Dev Ind Pharm, 26: 857-866.

Packer M., Bristow M. R., Cohn J. N., Colucci W. S., Fowler M. B., Gilbert E. M., Shusterman N. H. (1996) The Effect of Carvedilol on Morbidity and Mortality in Patients with Chronic Heart Failure. N Engl J Med, 334: 1349-1355.

Patel B. B., Patel J. K., Chakraborty S., Shukla D. (2015) Revealing facts behind spray dried solid dispersion technology used for solubility enhancement. Saudi Pharm J, 23: 352-365.

Patravale V. B., Date A. A., Kulkarni R. M. (2004) Nanosuspensions: a promising drug delivery strategy. J Pharm Parmacol, 56: 827-840.

Patterson J. E., James M. B., Forster A. H., Lancaster R. W., Butler J. M., Rades T. (2007) Preparation of glass solutions of three poorly water soluble drugs by spray drying, melt extrusion and ball milling. Int J Pharm, 336: 22-34.

Pelipenko J., Kocbek P., Kristl J. (2015) Critical attributes of nanofibers: Preparation, drug loading, and tissue regeneration. Int J Pharm, 484: 57-74.

Pelipenko J., Kristl J., Janković B., Baumgartner S., Kocbek P. (2013) The impact of relative humidity during electrospinning on the morphology and mechanical properties of nanofibers. Int J Pharm, 456: 125-134.

Pham Q. P., Sharma U., Mikos A. G. (2006) Electrospinning of polymeric nanofibers for tissue engineering applications: a review. Tissue Eng 12: 1197-1211.

Pham T. N., Watson S. A., Edwards A. J., Chavda M., Clawson J. S., Strohmeier M., Vogt F. G. (2010) Analysis of amorphous solid dispersions using 2D solid-state NMR and 1H T 1 relaxation measurements. Mol Pharm, 7: 1667-1691.

Pouton C. W. (2006) Formulation of poorly water-soluble drugs for oral administration: Physicochemical and physiological issues and the lipid formulation classification system. Eur J Pharm Sci, 29: 278-287.

Puhl S., Li L., Meinel L., Germershaus O. (2014) Controlled Protein Delivery from Electrospun Non-Wovens: Novel Combination of Protein Crystals and a Biodegradable Release Matrix. Mol Pharm, 11: 2372-2380.

Qi S., Belton P., Nollenberger K., Clayden N., Reading M., Craig D. M. (2010) Characterisation and Prediction of Phase Separation in Hot-Melt Extruded Solid Dispersions: A Thermal, Microscopic and NMR Relaxometry Study. Pharm Res, 27: 1869-1883.

Qian F., Huang J., Hussain M. A. (2010) Drug–polymer solubility and miscibility: Stability consideration and practical challenges in amorphous solid dispersion development. J Pharm Sci, 99: 2941-2947.

Rabinow B. E. (2004) Nanosuspensions in drug delivery. Nat Rev Drug Discov 3: 785-796.

Rao V. M., Sanghvi R., Zhu H. Solubility of Pharmaceutical Solids. In: Qiu, Y., Chen, Y., Zhang, G. G., Liu, L.,Porter, W. (ed.), Developing solid oral dosage forms: pharmaceutical theory & practice. Academic Press, Burlington, 2009:8-24.

Reddi A. H. (2000) Morphogenesis and tissue engineering of bone and cartilage: inductive signals, stem cells, and biomimetic biomaterials. Tissue Eng, 6: 351-359.

Repka M. A., Battu S. K., Upadhye S. B., Thumma S., Crowley M. M., Zhang F., Martin C., McGinity J. W. (2007) Pharmaceutical Applications of Hot-Melt Extrusion: Part II. Drug Dev Ind Pharm, 33: 1043-1057.

Rho K. S., Jeong L., Lee G., Seo B.-M., Park Y. J., Hong S.-D., Roh S., Cho J. J., Park W. H., Min B.-M. (2006) Electrospinning of collagen nanofibers: Effects on the behavior of normal human keratinocytes and early-stage wound healing. Biomaterials, 27: 1452-1461.

Risdian C., Nasir M., Rahma A., Rachmawati H. (2015) The Influence of Formula and Process on Physical Properties and the Release Profile of PVA/BSA Nanofibers Formed by Electrospinning Technique. J Nano Res, 31: 103-116.

Rowe R., Sheskey P., Owen S. Handbook of Pharmaceutical Excipients. Pharmaceutical Press, London, 2009: 317-322.

Ruffolo R., Jr., Feuerstein G. (1997) Pharmacology of Carvedilol: Rationale for Use in Hypertension, Coronary Artery Disease, and Congestive Heart Failure. Cardiovasc Drugs Ther, 11: 247-256.

Sarkar K., Gomez C., Zambrano S., Ramirez M., de Hoyos E., Vasquez H., Lozano K. (2010) Electrospinning to Forcespinning™. Mater Today, 13: 12-14.

Sarnes A., Kovalainen M., Häkkinen M. R., Laaksonen T., Laru J., Kiesvaara J., Ilkka J., Oksala O., Rönkkö S., Järvinen K., Hirvonen J., Peltonen L. (2014) Nanocrystal-based

per-oral itraconazole delivery: Superior in vitro dissolution enhancement versus Sporanox® is not realized in in vivo drug absorption. J Control Release, 180: 109-116.

Savjani K. T., Gajjar A. K., Savjani J. K. (2012) Drug Solubility: Importance and Enhancement Techniques. ISRN Pharm, 2012: 195727 (online).

Sebe I., Bodai Z., Eke Z., Kallai-Szabo B., Szabo P., Zelko R. (2014) Comparison of directly compressed vitamin B12 tablets prepared from micronized rotary-spun microfibers and cast films. Drug Dev Ind Pharm, 41: 1438-1442.

Sebe I., Kallai-Szabó B., Kovács K., Szabadi E., Zelkó R. (2015) Micro- and macrostructural characterization of polyvinylpirrolidone rotary-spun fibers. Drug Dev Ind Pharm, 41: 1829-1834.

Sebe I., Szabó B., Nagy Z. K., Szabó D., Zsidai L., Kocsis B., Zelkó R. (2013) Polymer structure and antimicrobial activity of polyvinylpyrrolidone-based iodine nanofibers prepared with high-speed rotary spinning technique. Int J Pharm, 458: 99-103.

Shoyele S. A., Cawthorne S. (2006) Particle engineering techniques for inhaled biopharmaceuticals. Adv Drug Deliver Rev, 58: 1009-1029.

Shukla S., Brinley E., Cho H. J., Seal S. (2005) Electrospinning of hydroxypropyl cellulose fibers and their application in synthesis of nano and submicron tin oxide fibers. Polymer (Guildf), 46: 12130-12145.

Sinha S., Ali M., Baboota S., Ahuja A., Kumar A., Ali J. (2010) Solid Dispersion as an Approach for Bioavailability Enhancement of Poorly Water-Soluble Drug Ritonavir. AAPS PharmSciTech, 11: 518-527.

Six K., Leuner C., Dressman J., Verreck G., Peeters J., Blaton N., Augustijns P., Kinget R., Van den Mooter G. (2002) Thermal Properties of Hot-Stage Extrudates of Itraconazole and Eudragit E100. Phase separation and polymorphism. J Therm Anal Calorim, 68: 591-601.

Six K., Verreck G., Peeters J., Brewster M., Mooter G. V. d. (2004) Increased physical stability and improved dissolution properties of itraconazole, a class II drug, by solid dispersions that combine fast- and slow-dissolving polymers. J Pharm Sci, 93: 124-131.

Song J.-H., Kim H.-E., Kim H.-W. (2008) Electrospun fibrous web of collagen–apatite precipitated nanocomposite for bone regeneration. J Mater Sci Mater Med, 19: 2925-2932.

Sonseca A., Peponi L., Sahuquillo O., Kenny J. M., Giménez E. (2012) Electrospinning of biodegradable polylactide/hydroxyapatite nanofibers: Study on the morphology, crystallinity structure and thermal stability. Polym Degrad Stab, 97: 2052-2059.

Squillante I., Emilio, Sethia S. (2003) Solid Dispersions: Revival with Greater Possibilities and Applications in Oral Drug Delivery. Crit Rev Ther Drug Carrier Syst, 20: 215-247.

Stegemann S., Leveiller F., Franchi D., de Jong H., Lindén H. (2007) When poor solubility becomes an issue: From early stage to proof of concept. Eur J Pharm Sci, 31: 249-261.

Stejskal E. O., Schaefer J., Sefcik M. D., McKay R. A. (1981) Magic-angle carbon-13 nuclear magnetic resonance study of the compatibility of solid polymeric blends. Macromolecules, 14: 275-279.

Stella V. J., Nti-Addae K. W. (2007) Prodrug strategies to overcome poor water solubility. Adv Drug Deliver Rev, 59: 677-694.

Szabó P., Kállai-Szabó B., Kállai-Szabó N., Sebe I., Zelkó R. (2014a) Preparation of hydroxypropyl cellulose microfibers by high-speed rotary spinning and prediction of the fiber-forming properties of hydroxypropyl cellulose gels by texture analysis. Cellulose, 21: 4419-4427.

Szabó P., Kállai-Szabó B., Sebe I., Zelkó R. (2014b) Preformulation study of fiber formation and formulation of drug-loaded microfiber based orodispersible tablets for in vitro dissolution enhancement. Int J Pharm, 477: 643-649.

Szabó P., Sebe I., Stiedl B., Kállai-Szabó B., Zelkó R. (2015) Tracking of crystalline-amorphous transition of carvedilol in rotary spun microfibers and their formulation to orodispersible tablets for in vitro dissolution enhancement. J Pharm Biomed Anal, 115: 359-367.

Szabó P., Zelkó R. (2015) Formulation and Stability Aspects of Nanosized Solid Drug Delivery Systems. Curr Pharm Des, 21: 3148-3157.

Taepaiboon P., Rungsardthong U., Supaphol P. (2006) Drug-loaded electrospun mats of poly (vinyl alcohol) fibres and their release characteristics of four model drugs. Nanotechnology, 17: 2317-2329.

Taylor L., Zografi G. (1997) Spectroscopic Characterization of Interactions Between PVP and Indomethacin in Amorphous Molecular Dispersions. Pharm Res, 14: 1691-1698.

Tennent H., Moy D., Niu C.-M. (2000) High surface area nanofibers, methods of making, methods of using and products containing same. Patent No. US6099960 A.

Teo W., Ramakrishna S. (2006) A review on electrospinning design and nanofibre assemblies. Nanotechnology, 17: 89-106.

Thakur R., Florek C., Kohn J., Michniak B. (2008) Electrospun nanofibrous polymeric scaffold with targeted drug release profiles for potential application as wound dressing. Int J Pharm, 364: 87-93.

Tian Y., Caron V., Jones D. S., Healy A.-M., Andrews G. P. (2014) Using Flory–Huggins phase diagrams as a pre-formulation tool for the production of amorphous solid dispersions: a comparison between hot-melt extrusion and spray drying. J Pharm Parmacol, 66: 256-274.

Um I. C., Fang D., Hsiao B. S., Okamoto A., Chu B. (2004) Electro-Spinning and Electro-Blowing of Hyaluronic Acid. Biomacromolecules, 5: 1428-1436.

v. Möllendorff E., Reiff K., Neugebauer G. (1987) Pharmacokinetics and bioavailability of carvedilol, a vasodilating beta-blocker. Eur J Clin Pharmacol, 33: 511-513.

van De Waterbeemd H., Smith D. A., Beaumont K., Walker D. K. (2001) Property-based design: optimization of drug absorption and pharmacokinetics. J Med Chem, 44: 1313-1333.

Vigh T., Horváthová T., Balogh A., Sóti P. L., Drávavölgyi G., Nagy Z. K., Marosi G. (2013) Polymer-free and polyvinylpirrolidone-based electrospun solid dosage forms for drug dissolution enhancement. Eur J Pharm Sci, 49: 595-602.

Wang J., Flanagan D. R. (1999) General solution for diffusion-controlled dissolution of spherical particles. 1. Theory. J Pharm Sci, 88: 731-738.

Wang J., Flanagan D. R. (2002) General solution for diffusion-controlled dissolution of spherical particles. 2. Evaluation of experimental data. J Pharm Sci, 91: 534-542.

Werbowyj R. S., Gray D. G. (1984) Optical properties of hydroxypropyl cellulose liquid crystals. I. Cholesteric pitch and polymer concentration. Macromolecules, 17: 1512-1520.

Weuts I., Kempen D., Decorte A., Verreck G., Peeters J., Brewster M., Van Den Mooter G. (2004) Phase behaviour analysis of solid dispersions of loperamide and two structurally related compounds with the polymers PVP-K30 and PVP-VA64. Eur J Pharm Sci, 22: 375-385.

Wu C.-Y., Benet L. Z. (2005) Predicting Drug Disposition via Application of BCS: Transport/Absorption/ Elimination Interplay and Development of a Biopharmaceutics Drug Disposition Classification System. Pharm Res, 22: 11-23.

Wu C.-Y., Benet L. Z., Hebert M. F., Gupta S. K., Rowland M., Gomez D. Y., Wacher V. J. (1995) Differentiation of absorption and first-pass gut and hepatic metabolism in humans: Studies with cyclosporine. Clin Pharmacol Ther, 58: 492-497.

Wu W., Nancollas G. (1998) A New Understanding of the Relationship Between Solubility and Particle Size. J Solution Chem, 27: 521-531.

Wu Y., Kesisoglou F. Immediate Release Oral Dosage Forms: Formulation Screening in the Pharmaceutical Industry. In: Dressman, J. B.,Reppas, C. (ed.), Oral drug absorption: Prediction and assessment. Informa Healthcare USA, New York, 2010:296-337.

Xie J., Michael P. L., Zhong S., Ma B., MacEwan M. R., Lim C. T. (2012) Mussel inspired protein-mediated surface modification to electrospun fibers and their potential biomedical applications. J Biomed Mater Res A, 100: 929-938.

Xie J., Wang C.-H. (2006) Electrospun Micro- and Nanofibers for Sustained Delivery of Paclitaxel to Treat C6 Glioma in Vitro. Pharm Res, 23: 1817-1826.

Xu S., Zhang J., He A., Li J., Zhang H., Han C. C. (2008) Electrospinning of native cellulose from nonvolatile solvent system. Polymer (Guildf), 49: 2911-2917.

Xu X., Yang Q., Wang Y., Yu H., Chen X., Jing X. (2006) Biodegradable electrospun poly(l-lactide) fibers containing antibacterial silver nanoparticles. Eur Polym J, 42: 2081-2087.

Yarin A. L. (2011) Coaxial electrospinning and emulsion electrospinning of core–shell fibers. Polym Adv Technol, 22: 310-317.

Yarin A. L., Koombhongse S., Reneker D. H. (2001) Taylor cone and jetting from liquid droplets in electrospinning of nanofibers. J Appl Phys, 90: 4836-4846.

Yoshioka M., Hancock B. C., Zografi G. (1994) Crystallization of indomethacin from the amorphous state below and above its glass transition temperature. J Pharm Sci, 83: 1700-1705.

You Y., Lee S. J., Min B. M., Park W. H. (2006) Effect of solution properties on nanofibrous structure of electrospun poly (lactic-co-glycolic acid). J Appl Polym Sci, 99: 1214-1221.

Yu D. G., Wang X., Li X. Y., Chian W., Li Y., Liao Y. Z. (2013) Electrospun biphasic drug release polyvinylpyrrolidone/ethyl cellulose core/sheath nanofibers. Acta Biomater, 9: 5665-5672.

Yu L., Bridgers A., Polli J., Vickers A., Long S., Roy A., Winnike R., Coffin M. (1999) Vitamin E-TPGS Increases Absorption Flux of an HIV Protease Inhibitor by Enhancing Its Solubility and Permeability1. Pharm Res, 16: 1812-1817.

Zema L., Loreti G., Melocchi A., Maroni A., Gazzaniga A. (2012) Injection Molding and its application to drug delivery. J Control Release, 159: 324-331.

Zeng J., Aigner A., Czubayko F., Kissel T., Wendorff J. H., Greiner A. (2005a) Poly(vinyl alcohol) Nanofibers by Electrospinning as a Protein Delivery System and the Retardation of Enzyme Release by Additional Polymer Coatings. Biomacromolecules, 6: 1484-1488.

Zeng J., Yang L., Liang Q., Zhang X., Guan H., Xu X., Chen X., Jing X. (2005b) Influence of the drug compatibility with polymer solution on the release kinetics of electrospun fiber formulation. J Control Release, 105: 43-51.

Zhang C., Yuan X., Wu L., Han Y., Sheng J. (2005a) Study on morphology of electrospun poly(vinyl alcohol) mats. Eur Polym J, 41: 423-432.

Zhang Y., Lim C. T., Ramakrishna S., Huang Z.-M. (2005b) Recent development of polymer nanofibers for biomedical and biotechnological applications. J Mater Sci Mater Med, 16: 933-946.

Zhao Q., Wang T., Wang J., Zheng L., Jiang T., Cheng G., Wang S. (2011) Template-directed hydrothermal synthesis of hydroxyapatite as a drug delivery system for the poorly water-soluble drug carvedilol. Appl Surf Sci, 257: 10126-10133.

Zhou D., Grant D. J. W., Zhang G. G. Z., Law D., Schmitt E. A. (2007) A calorimetric investigation of thermodynamic and molecular mobility contributions to the physical stability of two pharmaceutical glasses. J Pharm Sci, 96: 71-83.

DOI:10.14753/SE.2016.1927

11. LIST OF PUBLICATIONS

11.1. Publications relevant to the dissertation

1. **Szabó, P**., Kállai-Szabó, B., Kállai-Szabó, N., Sebe, I., Zelkó, R. (2014) Preparation of hydroxypropyl cellulose microfibers by high-speed rotary spinning and prediction of the fiber-forming properties of hydroxypropyl cellulose gels by texture analysis. Cellulose, 21: 4419-4427.
2. **Szabó, P.**, Kállai-Szabó, B., Sebe, I., Zelkó, R. (2014) Preformulation study of fiber formation and formulation of drug-loaded microfiber based orodispersible tablets for in vitro dissolution enhancement. International Journal of Pharmaceutics, 477: 643-649.
3. **Szabó, P**., Sebe, I., Stiedl, B., Kállai-Szabó, B., Zelkó, R. (2015) Tracking of crystalline-amorphous transition of carvedilol in rotary spun microfibers and their formulation to orodispersible tablets for in vitro dissolution enhancement. Journal of Pharmaceutical and Biomedical Analysis, 115: 359-367.
4. **Szabó, P**., Zelkó, R. (2015) Formulation and Stability Aspects of Nanosized Solid Drug Delivery Systems. Current Pharmaceutical Design, 21: 3148-3157.

11.2. Other publications

1. Sebe, I., Bodai, Z., Eke, Z., Kállai-Szabó, B., **Szabó, P.**, Zelkó, R. (2014) Comparison of directly compressed vitamin B12 tablets prepared from micronized rotary-spun microfibers and cast films. Drug Development and Industrial Pharmacy, 1-5.
2. Sebe, I., **Szabó, P.**, Kállai-Szabó, B., Zelkó, R. (2015) Incorporating small molecules or biologics into nanofibers for optimized drug release: A review. International Journal of Pharmaceutics, 494: 516-530.
3. **Szabó, P.**, Zelkó, R. (2015) Gyógyszerek vér-agy gáton történő átjuttatásának korszerű technológiai lehetőségei. Gyógyszerészet 5: 259-263.
4. **Szabó, P.**, Kovacs-Kiss, D., Zelkó, R. (2015) Nőgyógyászati célra szánt, hormontartalmú implantátumok fejlesztési lehetőségeinek áttekintése: irodalmi áttekintés. Acta Pharmaceutica Hungarica, 4: 131-138.

5. Kovács, G., Varga, D., Sebe, I., Hajdú, M., **Szabó, P.**, Ostorházi, E., Antal, I. Korszerű tartósítási módszer fejlesztése magisztrálisan előállítható műkönnyhöz. Acta Pharmaceutica Hungarica 4: 139-143.

DOI:10.14753/SE.2016.1927

12. ACKNOWLEDGEMENTS

Good teachers make the best of a pupil's means;
great teachers foresee a pupil's ends. /Maria Callas/

First of all, I would like to express my most heartfelt gratitude to my supervisor, Prof. Romána Zelkó for her endless support and encouragement to my Ph.D. study, for her patience, guidance and concern throughout the course of my research.

I owe my gratitude to Dr. Eszter Bohus, whose wise counsels immensely aided me to start and proceed my Ph.D. study.

Special thanks should be given to my colleagues; Dr. György Thaler, Dr. Attila Bódis and Dr. László Csernák at Gedeon Richter Plc.; and to Prof. Béla Noszál, the chairman of School of Pharmaceutical Sciences at School of Ph.D. Studies, who made my research work possible at the Semmelweis University within the framework of the Semmelweis University – Gedeon Richter Plc. collaboration agreement.

I would like to offer my gratitude to Dr. István Antal, director of Department of Pharmaceutics, who supported my work by enabling the availability of the instruments and methods located in the institute.

I must also acknowledge Dr. Barnabás Kállai-Szabó, Dr. Nikolett Kállai Szabó and István Sebe for their constructive suggestions and help provided in the experimental work.

I would also like to express my sincere appreciation and thanks to Dr. Attiláné Meskó for her expertise in statistical evaluation.

To Dr. Virág Szente, thanks for her assistance in facilitating the approval procedure of the manuscripts at Gedeon Richter Plc.

My special thanks are extended to my colleagues at University Pharmacy Department of Pharmacy Administration for their selfless support, and especially for Sándorné Schwáb, Dr. Eszter Kocsis and Istvánné Szász.

Last but not the least, I would like to express my deepest gratitude to my beloved family, for their continuous support throughout my education, and to my friends for their loyal encouragement.